cell death (5). Four splice variants that differ in GITR intracellular domain have been identified. These cytoplasmic distinctions may generate different signaling events, and one of them may encode a decoy receptor (6). Mouse macrophages express constitutive levels of GITR–GITR ligand (GITRL) and stimulation with soluble GITR (sGITR) leads to an increased production of nitric oxide (7), COX-2 (8), and MMP-9 (9). Macrophage stimulation with sGITR signals through the Rel–NFκB pathway, but it remains to be determined if sGITR is an agonist or antagonist of GITR signaling (10). In vitro studies using murine GITRL protein and GITRL transfectants demonstrate that GITR signaling can enhance or inhibit the proliferation of Ag-stimulated T helper 1, T helper 2, and naive $CD4^+$ T cells from TCR transgenic mice depending on the concentration of the cognate peptide, thus suggesting that GITR can function as a costimulatory receptor for TCR activation (11). Mice deficient for GITR have normal lymphoid and T cell development (12). However, experiments with $GITR^{-/-}$ T cells showed hyperproliferation to TCR stimulation, increased IL-2 production, increased IL-2 receptor α chain (CD25) expression, and increased susceptibility to activation-induced cell death (AICD) (12). The human GITRL has been detected in several tissues including ovary, testis, kidney, pancreas, PBLs, lymph nodes, and human umbilical vein endothelial cells (3, 4). Mouse GITRL expression has been demonstrated in macrophages, B cells, and both immature and mature dendritic cells (11, 13, 14). Stimulation with mitogens or LPS results in a temporary increase in the expression levels of GITRL, which is regulated by the transcription factor NF-1(11).

Mouse models for autoimmune disease suggest that GITR activation may break self-tolerance and induce autoimmunity presumably by inhibition of immunoregulatory T cell suppression (15, 16). In vivo administration of the agonist anti-GITR Ab, DTA-1, does not deplete GITR-expressing cells (15), but the mechanism by which immunoregulatory T cells are inhibited by GITR activation or the effect of GITR stimulation on other cell types such as B cells has not been defined. Apart from in vitro studies suggesting a costimulatory role for GITR in $CD4^+$ T cell activation (11, 15, 17, 18), the function of GITR on $CD4^+CD25^-$ and especially $CD8^+CD25^-$ remains largely unknown. Because GITR expression is up-regulated upon stimulation of T cells, we were interested in studying GITR expression and activation of alloreactive $CD4^+CD25^-$ and $CD8^+CD25^-$ T cells and its effects on the development of GVHD.

Materials and Methods

Reagents and Antibodies. The DTA-1 hybridoma was generated as described previously (15), and rat IgG control Ab was obtained from Anogen. Antimurine CD16/CD32 FcR block (2.4G2), TNFR1 (55R-593), TNF (MP6-XT3), and all of the following fluorochrome labeled and purified antibodies against murine Ag were obtained from BD Biosciences: CD4 (RM4-5), CD8 (53-6.7), CD62L (MEL-14), CD122 (TM-B1), CD44 (IM7), CD45R/B220 (RA3-6B2), Gr-1 (RB6-8C5), CD25 (PC61), CD69 (H1.2F3), H-2Kb (AF6-88.5), Ly 9.1 (30C7), Fas (JO2), FasL (MFL3), isotype controls; rat IgG2a-κ (R35-95), rat IgG2a-λ (B39-4), rat IgG2b (A95-1), hamster IgG group 1 liter (Ha4/8), streptavidin-FITC, -PE, and -PCP. Biotinylated anti-murine GITR (BAF524) was obtained from R&D Systems. Carboxyfluorescein succinimidyl ester (CFSE) was obtained from Molecular Probes.

In Vitro Assays. Tissue culture medium consisted of RPMI 1640 or DMEM supplemented with 10% heat inactivated FBS, 100 U/ml penicillin, 100 μg/ml streptomycin, 2 mM L-glutamine, and 50 μM of 2-mercaptoethanol (2-ME). For Ab stimulation, 1 μg/ml anti-CD3 and anti-CD28 was used. For proliferation assays, 10 μg/ml DTA-1 or rat IgG control Ab was used. T cells were purified, and 10^5 cells/well were incubated for 6 d with irradiated (2,000 cGy) splenocytes as stimulators (2×10^5 cells/well) in 96-well plates. Cultures were pulsed during the final 18 h with 1 μCi/well thymidine and harvested with Topcount Harvester (19). Cell proliferation was determined as counts per minute.

BMT and T Cell Purification. Female C57BL/6 ($H\text{-}2^b$), BALB/c ($H\text{-}2^k$), B10.BR ($H\text{-}2^k$), CBA/J($H\text{-}2^k$), *lpr* (B6.MRL-Fas^{lpr}), and C57BL/6 ($Ly5.1^+$) were obtained from The Jackson Laboratory. $GITR^{-/-}$ mice (C57BL/6 × 129/SvJ) were generated at Memorial Sloan-Kettering (12). All mice were used between 8–10 wk of age. BM cells were removed aseptically from femurs and tibias and depleted of T cells by incubation with anti-Thy-1.2 for 30 min at 4°C followed by incubation with Low-TOX-M rabbit complement (Cedarlane Laboratories) for 40 min at 37°C. Cells (5×10^6 BM cells without splenic T cells) were resuspended in DMEM (Life Technologies) and transplanted by tail vein infusion (0.25 ml total volume) into lethally irradiated recipients on day 0. On day 0, before transplantation, recipients received 900 cGy (BALB/c) or 1300 cGy (CBA/J) total body irradiation (^{137}Cs source) as a split dose with a 3-h interval between doses (to reduce gastrointestinal toxicity). T cells were obtained from spleens, purified over a nylon wool column, or positively selected with anti-CD5 magnetic beads. $CD4^+CD25^-$ and $CD8^+CD25^-$ T cells were purified with magnetic beads (~90% purity; Miltenyi Biotec) or sorted with Moflow (~98–99% purity; DakoCytomation). Experiments were performed with sorted fractions and confirmed with bead-purified T cells. In brief, $CD25^-$ T cells were obtained by negative selection of splenocytes treated with anti-CD25 PE-conjugated Ab and anti-PE microbeads. $CD4^+$ and $CD8^+$ fractions were separated by positive selection for anti-CD4 or anti-CD8 antibodies conjugated to microbeads. Mice were housed in sterilized micro-isolator cages and received normal chow and autoclaved hyperchlorinated drinking water (pH 3.0). All experiments were performed in accordance with our institutional guidelines.

Assessment of GVHD. The severity of GVHD was assessed with a clinical GVHD scoring system as described previously (20). In brief, mice were individually scored every week for five clinical parameters on a scale from zero to two: weight loss, posture, activity, fur, and skin. A clinical GVHD index was generated by summation of the five criteria scores (0–10). Survival was monitored daily. Animals with scores >5 were considered moribund and were killed. GVHD organ pathology for bowel (terminal ileum and ascending colon) and liver was assessed in a blinded fashion on formalin-preserved, paraffin-embedded, hematoxylin and eosin–stained histopathology sections with a semi-quantitative scoring system. In brief, bowel and liver were scored for 18–22 parameters associated with GVHD as described previously (21, 22).

CFSE Labeling. Cells were labeled with CFSE as described previously (23). In brief, T cells were incubated with CFSE at a final concentration of 2.5 μM in PBS at 37°C for 20 min. Cells were washed three times with PBS before i.v. injection.

Flow Cytometric Analysis. T cells were washed in FACS® buffer (PBS with 2% FBS and 0.1% sodium azide) and incubated for 15 min at 4°C with anti-CD16/CD32 FcR block. Subsequently, cells were incubated for 30 min at 4°C with antibodies and washed twice with FACS® buffer. Stained cells were resuspended in FACS® buffer and analyzed on a FACSCalibur™ flow cytometer (Becton Dickinson) with CELLQuest™ or Flowjo software (Treestar). For annexin V analysis, after cell surface staining, the stained cells were resuspended in 100 μl annexin V binding buffer and 5 μl annexin V Ab. After a 20-min incubation at room temperature in the dark, an additional 300 μl annexin V binding buffer was added, and the cells were analyzed.

ELISA. MLR supernatant IL-2 and IFNγ levels were performed according to the manufacturer's instructions with Quantikine M kits from R&D Systems.

DTA-1 Administration. For GVHD studies, DTA-1 and rat isotype control was administered by i.p. at days −1, 6, and 13 (1 mg/day). For adoptive transfer experiments with CFSE-labeled T cells, the antibodies were administered at day −1 (1 mg i.p.).

Online Supplemental Material. The opposite effects of GITR stimulation on $CD4^+CD25^-$ and $CD8^+CD25^-$ T cells remain even at different concentrations of DTA-1 Ab and are independent from the TNF–TNFR pathway. Supernatants from $CD4^+CD25^-$ T cells activated in the presence of GITR stimulation have decreased levels of IL-2 and IFNγ. Online supplemental material is available at http://www.jem.org/cgi/content/full/jem.20040116/DC1.

Results

Alloreactive $CD4^+$ and $CD8^+$ T Cells Up-regulate GITR. To assess whether activation of $CD4^+$ and $CD8^+$ T cells results in up-regulation of GITR expression, we analyzed GITR cell surface expression on activated (in vitro stimulation with anti-CD3 and anti-CD28 antibodies) and alloreactive (in vivo alloactivation after transfer into an allogeneic recipient) $CD4^+$ and $CD8^+$ T cells. In vitro stimulation with plate-bound anti-CD3/anti-CD28 antibodies of $CD4^+CD25^-$ and $CD8^+CD25^-$ T cells enhanced the expression of cell surface GITR, whereas freshly isolated immunoregulatory T cells had constitutive high levels of GITR (unpublished data). We used an MHC class I/II disparate model (C57BL/6→BALB/c) to analyze the expression of GITR on alloreactive T cells in vivo in two ways. First, we infused CFSE-labeled donor $CD3^+$ T cells into sublethally irradiated allogeneic and syngeneic recipients and recovered the cells from the spleen 3 d after infusion (Fig. 1 A). CFSE-labeled donor T cells from syngeneic recipients expressed low levels of cell surface GITR, in contrast with fast-dividing donor alloreactive T cells recovered from allogeneic recipients that had an activated phenotype ($CD25^+$ and $CD44^+$) and increased levels of GITR on their surface. Second, we infused T cell–depleted (TCD) allo-BM (C57BL/6 TCD-BM) and allogeneic T cells (C57BL/6) into lethally irradiated recipients (BALB/c), and after 9 d, determined the GITR expression on donor T cells from the spleens of these recipients (Fig. 1 B). We found that these (alloreactive) donor T cells indeed had an activated phenotype ($CD25^+$, $CD44^+$, and $CD62L^-$; unpublished data), and as expected, both $CD4^+$ and $CD8^+$ donor T cells had increased GITR expression. Therefore, we conclude that alloreactive $CD4^+$ and $CD8^+$ T cells up-regulate their GITR expression.

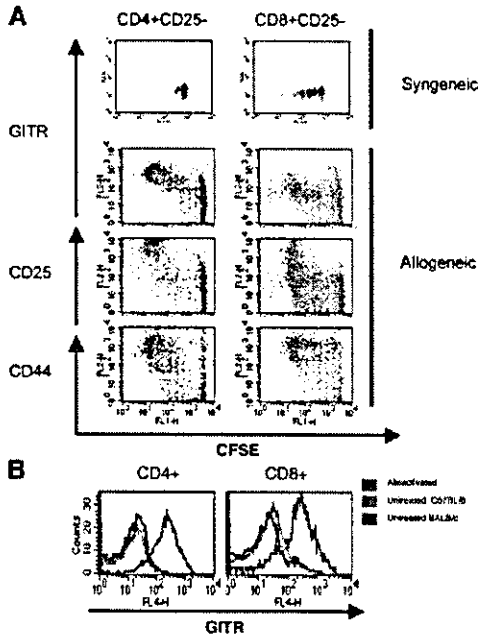

Figure 1. Alloactivation induces up-regulation of cell surface GITR on T cells. (A) Sublethally irradiated (750 cGy) syngeneic hosts (C57BL/6 Ly5.1) and allogeneic hosts (BALB/c) were infused with CFSE-labeled donor T cells (C57BL/6). GITR, CD25, and CD44 expression of these donor T cells was determined 3 d after infusion. (B) 9 d after BMT, GITR and CD25 expression was determined on splenic T cells from BALB/c recipients of C57BL/6 TCD-BM (5×10^6) and T cells (0.5×10^6), which were developing GVHD (red histogram). Blue histograms represent untransplanted controls (light blue, C57BL/6; dark blue, BALB/c).

Paradoxical Effect of GITR on $CD4^+CD25^-$ and $CD8^+$ $CD25^-$ T Cells. We studied the effects of GITR stimulation on alloreactive T cells using an anti-GITR agonist mAb (DTA-1) for in vitro and in vivo experiments. To exclude the previously described effects of GITR on immunoregulatory T cells (15), we used purified C57BL/6 $CD4^+CD25^-$ and $CD8^+CD25^-$ T cells as effectors in MLR experiments with MHC class I/II disparate irradiated stimulators (BALB/c; Fig. 2 A). Addition of DTA-1 to the MLR resulted in an ~2-fold decrease in proliferation of $CD4^+CD25^-$ T cells, whereas $CD8^+CD25^-$ T cell proliferation increased by ~3.5-fold when compared with addition of control Ab (Fig. 2 A, top). To eliminate potentially confounding variables associated with GITR expression on immunoregulatory T cells, B cells, and macrophages present in the splenocyte population used as stimulators, splenocytes isolated from $GITR^{+/-}$ and $GITR^{-/-}$ mice were tested as stimulators. Because these mice are on a

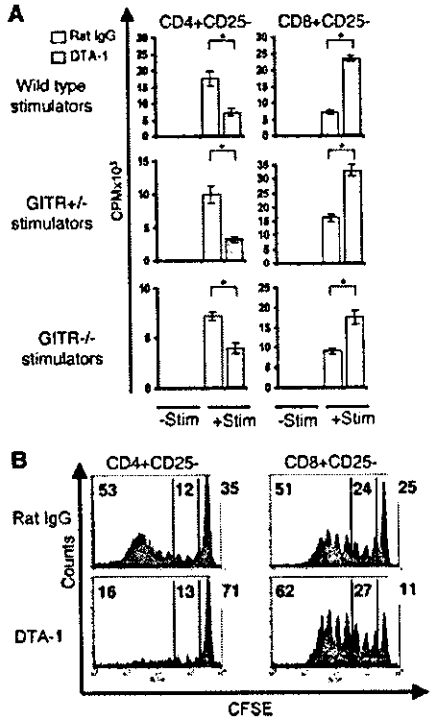

Figure 2. GITR stimulation induces paradoxical responses in $CD4^+$ $CD25^-$ and $CD8^+CD25^-$ T cells in vitro and in vivo. (A) An anti-GITR agonist Ab (DTA-1; 10 μg/ml) was added to MLRs of purified $CD4^+CD25^-$ and $CD8^+CD25^-$ splenic T cells as effector cells (10^5) with irradiated splenocytes as stimulators (2×10^5). (Wild-type stimulators) C57BL/6 effectors and BALB/c stimulators. ($GITR^{+/-}$ and $GITR^{-/-}$ stimulators) BALB/c effectors and $GITR^{+/-}$ or $GITR^{-/-}$ stimulators (C57BL/6 × 129/SvJ). −Stim, without stimulators. +Stim, with stimulators. *, $P < 0.001$. (B) Proliferative profile of recovered CFSE-labeled $CD4^+CD25^-$ and $CD8^+CD25^-$ T cells from sublethally irradiated hosts treated with 10 μg/ml DTA-1 or rat IgG control. These data are representative of three independent experiments. (top left) Percentage of alloreactive fast-proliferating donor T cells. (center) Percentage of slow proliferating donor T cells. (top right) Nondividing donor T cells.

mixed $H2^b$ background (C57BL/6 × 129/SvJ), we used purified $CD4^+CD25^-$ and $CD8^+CD25^-$ T cells from BALB/c mice as effectors (Fig. 2 A, bottom). Again, $CD4^+$ $CD25^-$ T cells showed decreased proliferation, whereas $CD8^+CD25^-$ T cell proliferation was enhanced by the addition of the DTA-1 Ab. Because this effect was observed using $GITR^{-/-}$ stimulators, we conclude that GITR stimulation via DTA-1 is independent of GITR expression on the stimulator population (including immunoregulatory T cells) and has a direct effect on $CD4^+CD25^-$ and $CD8^+CD25^-$ effector T cells. Also, this effect was not strain specific because results generated from T cells derived from C57BL/6 and BALB/c were consistent.

Our experiments clearly show inhibition of $CD4^+$ $CD25^-$ proliferation upon GITR stimulation, whereas other groups show enhancement of $CD4^+CD25^-$ T cell proliferation. Shimizu et al. (15) demonstrated that $CD4^+CD25^-$ T cells from $CD28^{-/-}$ were able to proliferate when stimulated via GITR. Tone et al. (11) showed that stimulation of GITR using a recombinant mouse GITRL could increase the proliferation of a Th2 clone through a wide range of cognate peptide concentration and a Th1 clone only at low peptide concentrations. Therefore, we analyzed whether the difference in proliferation of the alloreactive T cells could depend on the amount of anti-GITR agonist Ab present in the MLR. Because the Ag concentration is fixed (allorecognition), we titrated the anti-GITR Ab concentration over a 4-log range (Fig. S1, available at http://www.jem.org/cgi/content/full/jem.20040116/DC1). Addition of different concentrations spanning from 0.01 to 10 μg/ml of the GITR-stimulating Ab (DTA-1) to an MLR resulted again in decreased proliferation of $CD4^+CD25^-$ T cells and increased $CD8^+$ $CD25^-$ T cell proliferation.

Our data would suggest that $CD4^+CD25^-$ T cells from $GITR^{-/-}$ mice would show increased proliferation, whereas $CD8^+CD25^-$ T cells from $GITR^{-/-}$ mice would have impaired proliferative capacity. Ronchetti et al. (17) have shown that, indeed, upon anti-CD3 stimulation, $CD4^+$ but not the $CD8^+$ $GITR^{-/-}$ subpopulation had a higher proliferation rate than the $CD4^+$ $GITR^{+/+}$ subpopulation. Because T cell responses to Ab stimulation may be irrelevant to our model of allo-BMT, we tested the proliferative capacity of $GITR^{-/-}$ and $GITR^{+/-}$ T cells derived from mice of a mixed background (C57BL/6 × 129/SvJ). Our preliminary results indicate that there is no difference in $CD4^+CD25^-$ and $CD8^+CD25^-$ T cell proliferation upon allostimulation using third party stimulators (BALB/c; unpublished data). However, these experiments were performed with cells from $GITR^{-/-}$ and $GITR^{+/-}$ on a mixed background and we cannot rule out that genetic differences (other than the presence or absence of GITR) could have affected the alloresponse. Therefore, definitive experiments will have to be deferred until the $GITR^{-/-}$ mice have been completely backcrossed (>N 10).

To test whether the in vitro effects of anti-GITR agonist Ab (DTA-1) on alloreactive T cells were consistent in vivo, sublethally irradiated BALB/c mice were treated with DTA-1 or rat IgG control before adoptive transfer of C57BL/6 CFSE-labeled $CD4^+CD25^-$ or $CD8^+CD25^-$ T cells (Fig. 2 B). 3 d after T cell infusion, donor T cells were recovered and analyzed by flow cytometry. The in vivo proliferation profile of CFSE-labeled T cells allows the discrimination of slow proliferating cells, described in some models as homeostatic expansion, versus fast-dividing alloreactive T cells (24). GITR stimulation had no impact on the proportion of slow dividing $CD4^+CD25^-$ (12% in controls vs. 13% in DTA-1–treated recipients) and $CD8^+CD25^-$ (24 vs. 27%) T cells. However, GITR stimulation decreased the percentage of fast-dividing alloreactive $CD4^+CD25^-$ T cells (from 53 to 16%) and increased the percentage of fast-dividing alloreactive $CD8^+CD25^-$ T cells (from 51 to 62%). There were more nondividing $CD4^+CD25^-$ T cells in the DTA-1–treated group (71% in DTA-1–treated recipients vs. 35% in the controls), and

fewer nondividing $CD8^+CD25^-$ T cells in the DTA-1–treated group (11 vs. 25%) compared with the control Ab groups. These results indicate that GITR stimulation in vivo can inhibit alloreactive $CD4^+CD25^-$ expansion while it enhances alloreactive $CD8^+CD25^-$ expansion.

Fas–FasL Mediate GITR Inhibition of $CD4^+CD25^-$ T Cell Expansion. To determine if the Fas–FasL pathway was involved in GITR inhibition of $CD4^+CD25^-$ expansion, we studied the effect of GITR stimulation on cell surface expression of Fas and FasL (Fig. 3 A). $CD4^+CD25^-$ and $CD8^+CD25^-$ T cells allostimulated in the presence of the agonistic anti-GITR Ab (DTA-1) did not increase Fas expression nor was there a difference in FasL expression (unpublished data), although FasL cell surface expression is notoriously difficult to demonstrate by flow cytometric analysis. To address this question in a different assay, we studied the effect of DTA-1 on T cells from Fas-deficient *lpr* mice (Fig. 3 B). Addition of DTA-1 to an MLR had no effect on proliferation by *lpr* $CD4^+CD25^-$ T cells, in contrast with the inhibitory effect on wild-type $CD4^+CD25^-$ T cells. Alloreactive proliferation of both wild-type and *lpr* $CD8^+CD25^-$ T cells was increased when DTA-1 was added to the MLR. To demonstrate that GITR inhibition of $CD4^+CD25^-$ proliferation was due to FasL signaling, we studied the effect of anti-FasL blocking Ab during allostimulation (Fig. 3 C). As aforementioned, $CD4^+CD25^-$ T cell proliferation was impaired in the presence of DTA-1 while the addition of the FasL blocking Ab rescued $CD4^+CD25^-$ proliferation, although not completely. Because $CD4^+CD25^-$ proliferation is not completely restored after FasL blocking, other members of the TNFR family could be implicated. Proliferation of purified $CD4^+CD25^-$ T cells from $TNF^{-/-}$ and $TRAIL^{-/-}$ mice allostimulated in the presence of DTA-1 treatment remained impaired (Fig. 3 D). We further tested the role of TNFR1 by using an anti-TNFR1 blocking Ab. Proliferation of purified $CD4^+CD25^-$ T cells with TNFR1 and TNF blocking Ab in the presence of GITR stimulation still remained impaired (Fig. S2, available at http://www.jem.org/cgi/content/full/jem.20040116/DC1). These results show that GITR-mediated inhibition of $CD4^+CD25^-$ T cell expansion involves the Fas–FasL pathway and not the TNFR or TRAIL pathways, although the involvement of other members of the TNF family cannot be excluded.

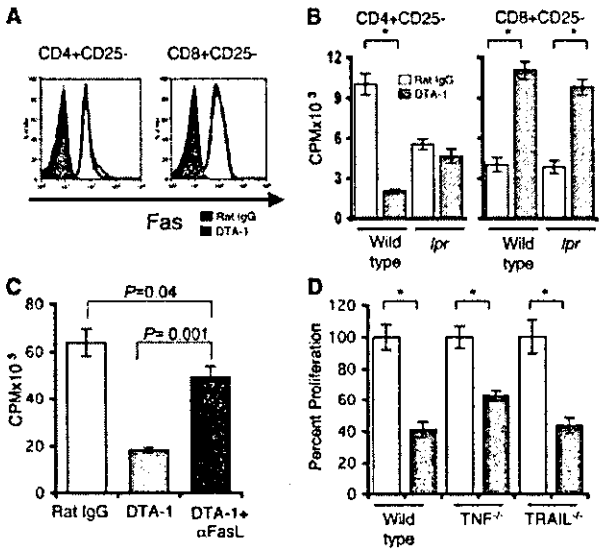

Figure 3. Fas–FasL pathway is involved in inhibition of $CD4^+CD25^-$ proliferation. (A) Fas expression was determined on purified C57BL/6 $CD4^+CD25^-$ and $CD8^+CD25^-$ T cells 72 h after anti-GITR agonist Ab (DTA-1) was added to MLRs with irradiated BALB/c stimulators. (shaded histograms) Isotype control. (blue histograms) Rat IgG–treated MLR. (red histograms) DTA-1–treated MLR. (B) DTA-1 was added to MLRs with purified $CD4^+CD25^-$ and $CD8^+CD25^-$ from *lpr* (B6.MRL-*Fas*^{lpr}) or wild-type (C57BL/6) mice as effectors and irradiated BALB/c splenocytes as stimulators. These data are representative of three experiments. *, $P < 0.001$. (C) Purified C57BL/6 $CD4^+CD25^-$ T cells were stimulated with irradiated BALB/c splenocytes in the presence of rat IgG control Ab, DTA-1 Ab, or DTA-1 plus MFL3, a FasL-blocking Ab. These data are representative of two independent experiments. (D) $CD4^+CD25^-$ T cells were purified from wild-type C57BL/6, C57BL/6-$TNF^{-/-}$, and C57BL/6 $TRAIL^{-/-}$ mice and stimulated with irradiated BALB/c splenocytes in the presence of rat IgG control Ab or DTA-1 Ab. (unshaded bars) Rat IgG treatment. (shaded bars) DTA-1 treatment. Results are presented as percent proliferation and are representative of two independent experiments. *, $P < 0.007$.

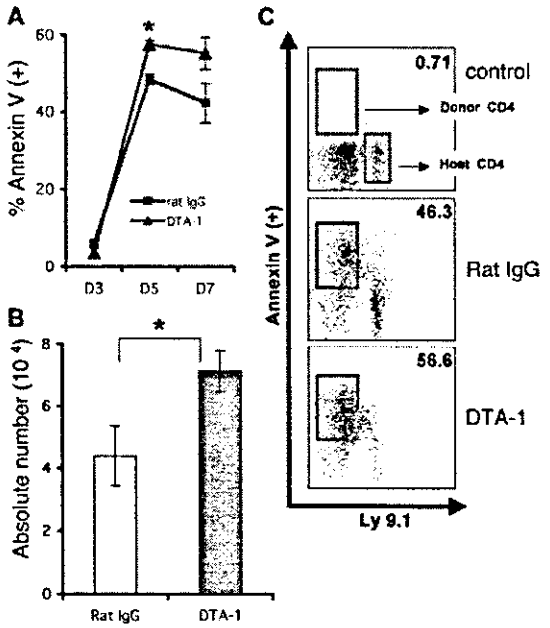

Figure 4. GITR stimulation induces early apoptosis of $CD4^+CD25^-$ alloreactive T cells after BMT. Lethally irradiated (900 cGy) BALB/c recipients of C57BL/6 TCD-BM and C57BL/6 $CD4^+CD25^-$ splenic T cells were treated with DTA-1 or control Ab (1 mg i.p. on days −1 and 6). Spleens were harvested on days 3, 5, and 7, and stained for annexin V (+) cells ($n = 3$ per group, per time point). (A) Time course of the percentage of donor-derived annexin V (+) cells is shown. *, $P = 0.0004$. (B) Absolute numbers of annexin V (+) donor $CD4^+$ T cells at day 5. *, $P = 0.05$. (C) Representative FACS® analyses of annexin V (+) donor and host $CD4^+$ T cells at day 7.

We measured the amount of IL-2 production of $CD4^+CD25^-$ T cells in the presence or absence of DTA-1 during allostimulation (Fig. S3, available at http://www.jem.org/cgi/content/full/jem.20040116/DC1). IL-2 was decreased in MLR supernatants of DTA-1–treated cocultures compared with control Ab–treated cocultures at days 2 and 5 of coculture (day 2, ~1.5 fold decrease and day 5, ~2.1-fold decrease). These decreased levels of IL-2 detected in our system may be a reflection of less viable $CD4^+CD25^-$ T cells.

These experiments indicate that GITR activation can initiate Fas-mediated AICD of alloreactive $CD4^+CD25^-$ T cells, whereas GITR stimulation of $CD8^+CD25^-$ T cell proliferation is independent of Fas–FasL signaling.

In Vivo GITR Stimulation Increases Apoptosis of $CD4^+$ $CD25^-$ Alloreactive T Cells. We wanted to address in our GVHD model if GITR stimulation increased $CD4^+CD25^-$ apoptosis in vivo. We infused 3×10^6 purified $CD4^+CD25^-$ T cells into lethally irradiated hosts treated with DTA-1 or rat IgG control Ab and determined apoptosis of donor T cells after 3, 5, and 7 d of allo-BMT (Fig. 4 A). Donor $CD4^+CD25^-$ T cells harvested from spleens of DTA-1–treated recipients showed increased annexin V staining when compared with donor T cells derived from control recipients treated with rat IgG (Fig. 4, B and C). We also studied the expression of activation markers at day 7 after BMT on $CD4^+CD25^-$ T cells from the DTA-1–treated group compared with the rat IgG–treated group and detected no significant difference in the level of CD25 and CD44 expression (unpublished data). These results indicate that DTA-1 treatment induces significantly more apoptosis of donor alloreactive $CD4^+CD25^-$ T cells early in the course of GVHD.

GITR Stimulation Modulates GVHD. In the C57BL/6→BALB/c strain combination, alloreactive $CD4^+$ T cells are more potent as GVHD effectors (25), whereas graft-versus-tumor activity is mostly dependent on alloreactive $CD8^+$ T cells (26). We used this model to determine the effects of anti-GITR agonistic Ab (DTA-1) on alloreactive $CD4^+CD25^-$ and $CD8^+CD25^-$ T cells during the development of GVHD. Pilot experiments determined that DTA-1 administration beginning at day −1 was optimal. The dose and schedule were consistent with previous papers in which anti-GITR antibodies have been used in vivo (weekly administration of 1 mg i.p.; references 16, 27).

We hypothesized that DTA-1 administration to allo-BMT recipients could ameliorate GVHD mediated by $CD4^+CD25^-$ T cells due to enhanced AICD of alloreactive T cells and aggravate GVHD mediated by $CD8^+CD25^-$ T cells due to their enhanced proliferation by GITR stimulation. Indeed, we observed that DTA-1–treated recipients of $CD4^+CD25^-$ C57BL/6 donor T cells, although not free of disease, had a significant delay and decrease in GVHD morbidity and mortality compared with recipients treated with a control Ab (Fig. 5, left).

Although alloreactive $CD4^+CD25^-$ cells are more potent on a per cell basis in the C57BL/6→BALB/c model,

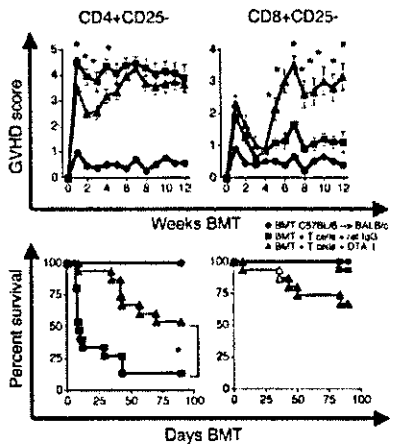

Figure 5. GITR stimulation decreases GVHD mediated by $CD4^+CD25^-$ cells and increases GVHD mediated by $CD8^+CD25^-$ T cells. Lethally irradiated (900 cGy) BALB/c recipients of C57BL/6 TCD-BM and C57BL/6 $CD4^+CD25^-$ or $CD8^+CD25^-$ splenic T cells were treated with DTA-1 Ab (1 mg i.p. on days −1, 6, and 13) or control Ab. (top) Mean ± SEM clinical GVHD scores. (bottom) Kaplan-Meier survival curves. Data shown are combined from three experiments, $n = 15$ per group. *, $P \leq 0.01$.

this strain combination has a class I and class II disparity, and $CD8^+CD25^-$ can induce GVHD. In other GVHD models with full MHC disparity, $CD8^+$-mediated GVHD can always be demonstrated (28). DTA-1–treated recipients of donor BM and donor $CD8^+CD25^-$ T cells had significantly increased GVHD morbidity and mortality (Fig. 5, right). Additional experiments in a MHC-matched strain combination in which GVHD is primarily dependent on alloreactive $CD8^+$ T cells (B10.BR→CBA/J) demonstrated that DTA-1 administration to allo-BMT recipients could aggravate GVHD (unpublished data). However, these mice were infused with unfractionated donor splenocytes; thus, increased mortality could also be due to the inhibition of suppressor function via GITR stimulation (15, 16) independent of its effect on $CD8^+$ donor T cells.

To further assess GVHD, target organ histopathology was studied (Fig. 6). Mice transplanted and infused with donor $CD4^+CD25^-$ donor T cells were killed at day 21 (Fig. 6 A). We lowered the dose of donor $CD4^+CD25^-$ T cells to 0.3×10^6 and delayed the time of organ harvest to day 21 due to high mortality in the rat IgG control group (Fig. 5). We observe significantly less GVHD target organ damage in liver and intestines of DTA-1–treated recipients compared with control recipients of $CD4^+CD25^-$ T cells. There was greater thymic cellularity in DTA-1–treated recipients, which is consistent with less thymi damage. Also, higher numbers of granulocytes were detected, consistent with less GVHD-associated myelosuppression. Mice transplanted and infused with $CD8^+CD25^-$ donor T cells were killed, and organs were harvested at day 55, when differences in clinical scores were more pronounced (Fig. 6 B). Consistent with our previous results, GITR stimulation of

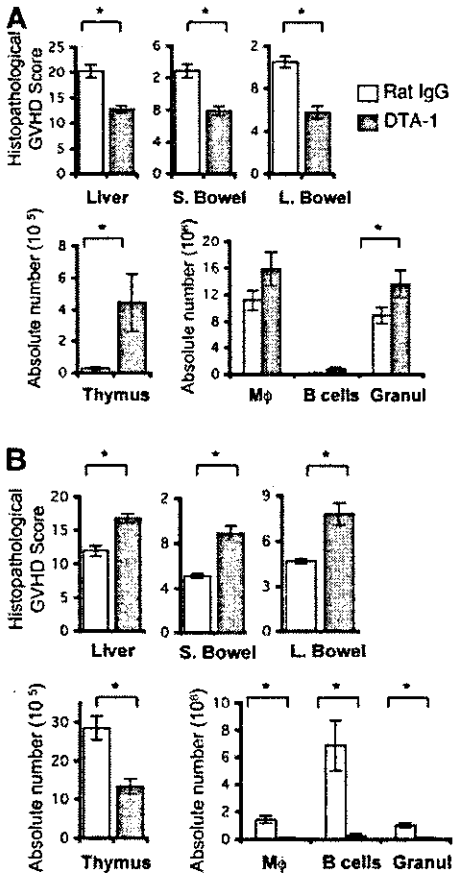

Figure 6. GITR stimulation decreases GVHD-associated organ damage mediated by $CD4^+CD25^-$ T cells and increases GVHD-associated organ damage mediated by $CD8^+CD25^-$ T cells. Lethally irradiated (900 cGy) BALB/c recipients of C57BL/6 TCD-BM and C57BL/6 $CD4^+CD25^-$ cells or $CD8^+CD25^-$ splenic T cells were treated with DTA-1 Ab or control Ab (1 mg i.p. on days −1, 6, and 13). Recipients of $CD4^+CD25^-$ T cells were killed, and organs were harvested on day 21 (A). Recipients of $CD8^+CD25^-$ T cells were killed, and organs were harvested on day 55 (B). (top) A semi-quantitative histopathological analysis for GVHD in liver, small bowel, and large bowel. (bottom left) The absolute number of thymocytes. (bottom right) The absolute numbers of splenic Mac-1^+ (Mϕ), B cells, and granulocytes (Granul) were analyzed by flow cytometry. Data shown are representative of one experiment, n = 9–10 per group. *, $P \leq 0.05$.

donor $CD8^+CD25^-$ donor T cells resulted in increased target organ damage and myelosuppression.

Discussion

Previous experiments have indicated that in vitro stimulation of GITR on immunoregulatory T cells inhibits their suppressive effect and that in vivo GITR stimulation induced development of autoimmunity presumably due to immunoregulatory T cell inhibition (15, 16). The effects of GITR stimulation on $CD4^+$ and $CD8^+$ have not been fully addressed, especially in vivo. Here, we demonstrate that GITR stimulation in vitro and in vivo has an important role in the costimulation of alloreactive $CD4^+CD25^-$ and $CD8^+CD25^-$ T cells independent of its effect on immunoregulatory T cells. Stimulation with a GITR-activating Ab inhibited $CD4^+CD25^-$ proliferation and decreased GVHD, whereas it enhanced alloreactive $CD8^+CD25^-$ T cell proliferation and increased GVHD. Our data indicate that GITR-mediated inhibition of $CD4^+CD25^-$ T cell expansion involves the Fas–FasL pathway, suggesting that GITR activation can initiate Fas-mediated AICD of alloreactive $CD4^+CD25^-$ T cells, whereas GITR stimulation of $CD8^+CD25^-$ T cell proliferation is independent of Fas–FasL signaling. Our results are consistent with the notion that GITR stimulation could lower the threshold for T cell activation inducing increased AICD in $CD4^+CD25^-$, but not in $CD8^+CD25^-$ T cells, where it induces proliferation. Thus, GITR stimulation of alloreactive $CD4^+CD25^-$ T cells in vivo can provide a novel strategy to prevent or treat GVHD.

Other laboratories have described GITR signaling as costimulatory for CD4 and CD8 (15, 17). Experiments using polyclonal stimulation with low concentrations of plate-bound or soluble anti-CD3 Ab (0.1–0.5 μg/ml; references 15, 17, 18) demonstrate that anti-GITR increases proliferation, but in some experiments, this costimulation is lost at higher concentrations of anti-CD3 Ab (1–3 μg/ml; references 15, 18). Our experiments addressing the role of GITR stimulation using Ab stimulation showed no difference in the proliferation of $CD4^+CD25^-$ cells stimulated with 10 μg/ml of soluble anti-CD3 and soluble anti-GITR agonistic Ab (DTA-1). $CD8^+CD25^-$ T cell proliferation under the same conditions was slightly increased (unpublished data). However, experiments addressing the effects of GITR stimulation upon Ag-specific recognition, a more representative model of allo-specific responses, show results consistent with ours. Because GVHD is a Th1-mediated complication of BMT (29, 30), experiments by Tone et al. (11) with a Th1 clone derived from TCR transgenic mice using a rGITRL for GITR stimulation are more relevant to our model. When the Th1 clone is stimulated with a low concentration of the cognate peptide (1 nM), rGITRL proliferation is enhanced. In contrast, when the Th1 clone is stimulated in the presence of rGITRL and higher peptide concentrations (10–100 nM), proliferation is inhibited. The same results were observed using naive T cells derived from the same transgenic mice where the presence of GITR stimulation at high peptide concentrations inhibited proliferation (11).

Furthermore, Shimizu et al. (15) have shown that xenostimulated $CD4^+CD25^-$ T cells have decreased proliferation in the presence of anti-GITR agonistic Ab (DTA-1). Murine $CD4^+CD25^-$ T cells were stimulated with rat APCs. The authors demonstrate that DTA-1 has no cross-reactivity with rat APCs, indicating that any effect observed by the addition of the agonist Ab will be a result of its direct effect on the murine cells. When $CD4^+CD25^-$ T cells were xenostimulated in the presence of a control Ab, they proliferate extensively, whereas addition of DTA-1 to the same culture resulted in a marked decrease in proliferation.

These experiments that analyze Ag-dependent T cell activation are very similar to our results, suggesting that during allo- and xenostimulation the addition of GITR stimulation may induce a potent costimulation, which can inhibit proliferation at higher Ag concentration. Our experiments indicate that this inhibitory effect on proliferation could be due to AICD.

We believe that the overall effect of in vivo GITR stimulation needs to be reconsidered because GITR stimulation can have a differential and/or paradoxical effect on regulatory T cells, $CD4^+$ effector T cells, and $CD8^+$ effector T cells. Our data in clinically relevant models for GVHD suggest that in vivo GITR stimulation holds therapeutic promise for the separation of CD8-mediated graft-versus-tumor activity from CD4-mediated GVHD activity.

S.J. Muriglan would like to dedicate this paper to Donald Holmquist.

A.N. Houghton and T. Ramirez-Montagut were supported by the National Institutes of Health (grants CA59350, CA58621, and CA33049) and Swim Across America. This work was supported by RO1 grants HL69929 and HL72412 from the National Institutes of Health (to M.R.M. van den Brink). M.R.M. van den Brink is the recipient of a Damon Runyon Scholar Award of the Cancer Research Fund.

Submitted: 20 January 2004
Accepted: 28 May 2004

References

1. Nocentini, G., L. Giunchi, S. Ronchetti, L.T. Krausz, A. Bartoli, R. Moraca, G. Migliorati, and C. Riccardi. 1997. A new member of the tumor necrosis factor/nerve growth factor receptor family inhibits T cell receptor-induced apoptosis. *Proc. Natl. Acad. Sci. USA.* 94:6216–6221.
2. Nocentini, G., A. Bartoli, S. Ronchetti, L. Giunchi, A. Cupelli, D. Delfino, G. Migliorati, and C. Riccardi. 2000. Gene structure and chromosomal assignment of mouse GITR, a member of the tumor necrosis factor/nerve growth factor receptor family. *DNA Cell Biol.* 19:205–217.
3. Gurney, A.L., S.A. Marsters, R.M. Huang, R.M. Pitti, D.T. Mark, D.T. Baldwin, A.M. Gray, A.D. Dowd, A.D. Brush, A.D. Heldens, et al. 1999. Identification of a new member of the tumor necrosis factor family and its receptor, a human ortholog of mouse GITR. *Curr. Biol.* 9:215–218.
4. Kwon, B., K.Y. Yu, J. Ni, G.L. Yu, I.K. Jang, Y.J. Kim, L. Xing, D. Liu, S.X. Wang, and B.S. Kwon. 1999. Identification of a novel activation-inducible protein of the tumor necrosis factor receptor superfamily and its ligand. *J. Biol. Chem.* 274:6056–6061.
5. Spinicelli, S., G. Nocentini, S. Ronchetti, L.T. Krausz, R. Bianchini, and C. Riccardi. 2002. GITR interacts with the pro-apoptotic protein Siva and induces apoptosis. *Cell Death Differ.* 9:1382–1384.
6. Nocentini, G., S. Ronchetti, A. Bartoli, S. Spinicelli, D. Delfino, L. Brunetti, G. Migliorati, and C. Riccardi. 2000. Identification of three novel mRNA splice variants of GITR. *Cell Death Differ.* 7:408–410.
7. Shin, H.H., M.H. Lee, S.G. Kim, Y.H. Lee, B.S. Kwon, and H.S. Choi. 2002. Recombinant glucocorticoid induced tumor necrosis factor receptor (rGITR) induces NOS in murine macrophage. *FEBS Lett.* 514:275–280.
8. Shin, H.H., B.S. Kwon, and H.S. Choi. 2002. Recombinant glucocorticoid induced tumour necrosis factor receptor (rGITR) induced COX-2 activity in murine macrophage Raw 264.7 cells. *Cytokine.* 19:187–192.
9. Lee, H.S., H.H. Shin, B.S. Kwon, and H.S. Choi. 2003. Soluble glucocorticoid-induced tumor necrosis factor receptor (sGITR) increased MMP-9 activity in murine macrophage. *J. Cell. Biochem.* 88:1048–1056.
10. Shin, H.H., H.W. Lee, and H.S. Choi. 2003. Induction of nitric oxide synthase (NOS) by soluble glucocorticoid induced tumor necrosis factor receptor (sGITR) is modulated by IFN-gamma in murine macrophage. *Exp. Mol. Med.* 35:175–180.
11. Tone, M., Y. Tone, E. Adams, S.F. Yates, M.R. Frewin, S.P. Cobbold, and H. Waldmann. 2003. Mouse glucocorticoid-induced tumor necrosis factor receptor ligand is costimulatory for T cells. *Proc. Natl. Acad. Sci. USA.* 100:15059–15064.
12. Ronchetti, S., G. Nocentini, C. Riccardi, and P.P. Pandolfi. 2002. Role of GITR in activation response of T lymphocytes. *Blood.* 100:350–352.
13. Yu, K.Y., H.S. Kim, S.Y. Song, S.S. Min, J.J. Jeong, and B.S. Youn. 2003. Identification of a ligand for glucocorticoid-induced tumor necrosis factor receptor constitutively expressed in dendritic cells. *Biochem. Biophys. Res. Commun.* 310:433–438.
14. Kim, J.D., B.K. Choi, J.S. Bae, U.H. Lee, I.S. Han, H.W. Lee, B.S. Youn, D.S. Vinay, and B.S. Kwon. 2003. Cloning and characterization of GITR ligand. *Genes Immun.* 4:564–569.
15. Shimizu, J., S. Yamazaki, T. Takahashi, Y. Ishida, and S. Sakaguchi. 2002. Stimulation of CD25(+)CD4(+) regulatory T cells through GITR breaks immunological self-tolerance. *Nat. Immunol.* 3:135–142.
16. Uraushihara, K., T. Kanai, K. Ko, T. Totsuka, S. Makita, R. Iiyama, T. Nakamura, and M. Watanabe. 2003. Regulation of murine inflammatory bowel disease by CD25+ and CD25- CD4+ glucocorticoid-induced TNF receptor family-related gene+ regulatory T cells. *J. Immunol.* 171:708–716.
17. Ronchetti, S., O. Zollo, S. Bruscoli, M. Agostini, R. Bianchini, G. Nocentini, E. Ayroldi, and C. Riccardi. 2004. GITR, a member of the TNF receptor superfamily, is costimulatory to mouse T lymphocyte subpopulations. *Eur. J. Immunol.* 34:613–622.
18. Kohm, A.P., J.S. Williams, and S.D. Miller. 2004. Cutting edge: ligation of the glucocorticoid-induced TNF receptor enhances autoreactive CD4(+) T cell activation and experimental autoimmune encephalomyelitis. *J. Immunol.* 172:4686–4690.
19. Alpdogan, O., S.J. Muriglan, B.J. Kappel, E. Doubrovina, C. Schmaltz, R. Schiro, J.M. Eng, A.S. Greenberg, L.M. Willis, J.A. Rotolo, et al. 2003. Insulin-like growth factor-I enhances lymphoid and myeloid reconstitution after allogeneic bone marrow transplantation. *Transplantation.* 75:1977–1983.
20. Cooke, K.R., L. Kobzik, T.R. Martin, J. Brewer, J. Delmonte, Jr., J.M. Crawford, and J.L. Ferrara. 1996. An experimental model of idiopathic pneumonia syndrome after bone marrow transplantation: I. The roles of minor H antigens and endotoxin. *Blood.* 88:3230–3239.
21. Crawford, J.M. 1997. Graft-versus-host disease of the liver. *In* Graft-vs.-Host Disease. J.L.M. Ferrara, H.J. Deeg, and S.J. Burakoff, editors. Marcel Dekker, New York. 315–336.
22. Hill, G.R., J.M. Crawford, K.R. Cooke, Y.S. Brinson, L. Pan, and J.L. Ferrara. 1997. Total body irradiation and acute graft-versus-host disease: the role of gastrointestinal damage and inflammatory cytokines. *Blood.* 90:3204–3213.

23. Lyons, A.B., and C.R. Parish. 1994. Determination of lymphocyte division by flow cytometry. *J. Immunol. Methods.* 171:131–137.
24. Alpdogan, O., S.J. Muriglan, J.M. Eng, L.M. Willis, A.S. Greenberg, B.J. Kappel, and M.R. van den Brink. 2003. IL-7 enhances peripheral T cell reconstitution after allogeneic hematopoietic stem cell transplantation. *J. Clin. Invest.* 112: 1095–1107.
25. Hoffmann, P., J. Ermann, M. Edinger, C.G. Fathman, and S. Strober. 2002. Donor-type $CD4^+CD25^+$ regulatory T cells suppress lethal acute graft-versus-host disease after allogeneic bone marrow transplantation. *J. Exp. Med.* 196:389–399.
26. Edinger, M., P. Hoffmann, J. Ermann, K. Drago, C.G. Fathman, S. Strober, and R.S. Negrin. 2003. CD4+CD25+ regulatory T cells preserve graft-versus-tumor activity while inhibiting graft-versus-host disease after bone marrow transplantation. *Nat. Med.* 9:1144–1150.
27. Shimizu, J., and E. Moriizumi. 2003. CD4+CD25− T cells in aged mice are hyporesponsive and exhibit suppressive activity. *J. Immunol.* 170:1675–1682.
28. Schmaltz, C., O. Alpdogan, K.J. Horndasch, S.J. Muriglan, B.J. Kappel, T. Teshima, J.L. Ferrara, S.J. Burakoff, and M.R. van den Brink. 2001. Differential use of Fas ligand and perforin cytotoxic pathways by donor T cells in graft-versus-host disease and graft-versus-leukemia effect. *Blood.* 97:2886–2895.
29. Krenger, W., and J.L. Ferrara. 1996. Graft-versus-host disease and the Th1/Th2 paradigm. *Immunol. Res.* 15:50–73.
30. Krenger, W., G.R. Hill, and J.L. Ferrara. 1997. Cytokine cascades in acute graft-versus-host disease. *Transplantation.* 64: 553–558.

The origin of *FOXP3*-expressing CD4$^+$ regulatory T cells: thymus or periphery

Shimon Sakaguchi

Department of Experimental Pathology, Institute for Frontier Medical Sciences, Kyoto University, Kyoto, Japan
Laboratory for Immunopathology, RIKEN Research Center for Allergy and Immunology, Yokohama, Japan

Naturally arising CD4$^+$ regulatory T cells, which engage in the maintenance of immunologic self-tolerance, specifically express *FOXP3*, which encodes a transcription-repressor protein. Genetic defects in *FOXP3* cause IPEX, an X-linked autoimmune/inflammatory syndrome. With *FOXP3* as a specific marker for regulatory CD4$^+$ T cells in humans, it is now possible to determine their origin and developmental pathway (see the related article beginning on page 1437).

J. Clin. Invest. 112:1310–1312 (2003). doi:10.1172/JCI200320274.

The immune system discriminates between self and non-self, maintaining immunologic self-tolerance (i.e., unresponsiveness to self-constituents). It is known that potentially hazardous self-reactive T and B cells are clonally deleted at immature stages of their development or inactivated upon encounter with self-antigens in the periphery. There is now accumulating evidence that, in addition to these passive mechanisms of self-tolerance, a population of CD4$^+$ T cells, called regulatory T cells (T_R cells), engage in the maintenance of peripheral self-tolerance by actively suppressing the activation and expansion of self-reactive T cells (1–3). The majority, if not all, of such naturally occurring CD4$^+$ T_R cells constitutively express CD25 (IL-2 receptor α chain) in the physiologic state. Indeed, removal of CD25$^+$CD4$^+$ T cells, which constitute 5–10% of CD4$^+$ T cells in rodents and humans, leads to spontaneous development of various autoimmune diseases in otherwise normal mice (4). The removal of CD25$^+$CD4$^+$ T_R cells also triggers excessive or misdirected immune responses to microbial antigens, causing immunopathology, such as inflammatory bowel disease (IBD), due to hyper-reaction of the remaining T cells to commensal bacteria in the intestine (3).

Address correspondence to: Shimon Sakaguchi, Department of Experimental Pathology, Institute for Frontier Medical Sciences, Kyoto University, 53 Shogin Kawahara-cho, Sakyo-ku, Kyoto 606-8507, Japan. Phone: 81-75-751-3888; Fax: 81-75-751-3820; E-mail: shimon@frontier.kyoto-u.ac.jp.

Conflict of interest: The author has declared that no conflict of interest exists.

Nonstandard abbreviations used: regulatory T (T_R); inflammatory bowel disease (IBD); T cell receptor (TCR).

FOXP3: master control gene for the development and function of natural CD4$^+$ T_R cells

There is now evidence not only for the presence of CD25$^+$CD4$^+$ T_R cells in humans but also for their essential roles in controlling autoimmunity, immunopathology, and allergy in human diseases (5). This is best illustrated by IPEX (immune dysregulation, polyendocrinopathy, enteropathy, X-linked syndrome), a rare monogenic disease of male children that is accompanied by autoimmune disease (such as type 1 diabetes), IBD, and severe allergy similar to those produced in mice by depletion of CD25$^+$CD4$^+$ T_R cells (6). The causative gene, *FOXP3* (*Foxp3* in mice), which encodes a transcription repressor (7–10), is specifically expressed in CD25$^+$CD4$^+$ T cells in the thymus and periphery (11–13). Forced expression of the *Foxp3* gene can convert murine naive T cells to T_R cells that phenotypically and functionally resemble naturally arising CD25$^+$CD4$^+$ T_R cells (11, 12). Furthermore, inoculation of CD25$^+$CD4$^+$ T cells prepared from normal mice can prevent autoimmune disease in *Foxp3*-defective mice (12). These findings collectively indicate that *FOXP3* is a master control gene for the development and function of natural CD25$^+$CD4$^+$ T_R cells.

The origin and the developmental pathway of *FOXP3*-expressing T_R cells

The discovery of *FOXP3/Foxp3* as a specific and stable marker for natural T_R cells now makes it possible to determine the origin and the developmental pathway of T_R cells in humans, as reported by Walker et al. in this issue of the *JCI* (14). It has been shown, mainly in rodents, that the normal thymus continuously produces CD25$^+$CD4$^+$ T_R cells as a functionally mature T cell subpopulation that recognizes a broad repertoire of self- and non-self antigens, and that abrogation of the thymic production of T_R cells leads to the development of autoimmune disease (1–3). Walker et al. (14) show that CD25$^+$CD4$^+$ T cells in the peripheral blood lymphocytes express *FOXP3* and are capable of suppressing the activation and expansion of other T cells in vitro, as shown in rodents (11–13). Furthermore, they show that, in contrast with murine *Foxp3* expression, activation of CD25$^-$CD4$^+$ T cells by T cell receptor (TCR) stimulation induces *FOXP3* expression, and that *FOXP3*-expressing T cells derived from CD25$^-$CD4$^+$ T cells are equally as suppressive as natural CD25$^+$CD4$^+$ T_R cells (Figure 1) (14). This interesting finding suggests two possibilities regarding the origin of CD25$^+$CD4$^+$ T_R cells. One is that naive T cells can differentiate to CD25$^+$CD4$^+$ T_R cells upon TCR stimulation, in a manner similar to that in which the expression of the transcription factors T-bet and GATA-3 instruct naive T cells to differentiate to Th1 and Th2 cells, respectively (15, 16). Another possibility is that some of the functionally mature T_R cells pro-

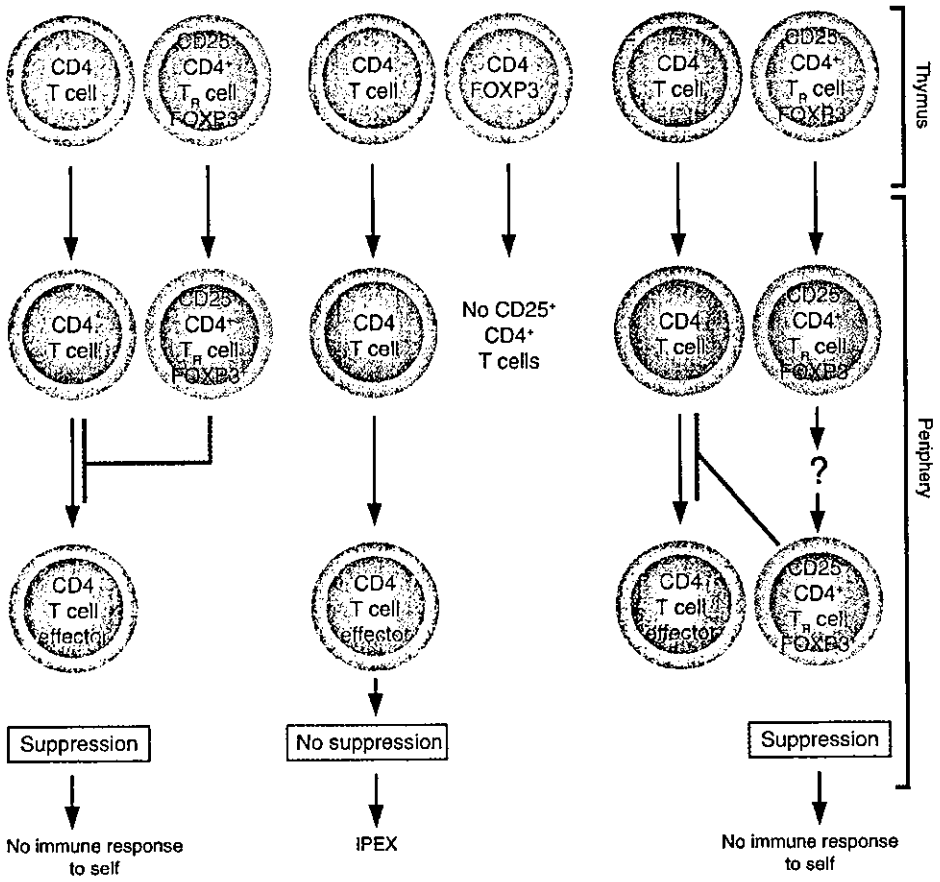

Figure 1
The normal thymus produces *FOXP3*-expressing CD25⁺CD4⁺ T_R cells. Some of the naive CD25⁻CD4⁺ T cells may also differentiate to *FOXP3*-expressing CD25⁺CD4⁺ T_R cells in the periphery. These T_R cells suppress the activation and expansion of self-reactive T cells that may cause autoimmune disease. Genetic defects of *FOXP3* cause IPEX due to developmental or functional defects of T_R cells. Adapted with permission from *Nature Immunology* (21).

duced by the thymus are CD25⁻ or lose CD25 expression with retention of their suppressive function, as has been shown in rodents (17–19). Such CD25⁻ T_R cells may become CD25⁺ upon activation, especially when other T cells respond to antigen stimulation, and IL-2 secreted by them may trigger the expansion of T_R cells. Given the specific expression of *FOXP3* in T_R cells whether they are of thymic or peripheral origin, it remains to be determined whether other T cells with regulatory functions, such as IL-10–secreting Tr1 or TGF-β–secreting Th3 cells, may also express *FOXP3* (20).

Besides self-tolerance and autoimmunity, evidence is now accumulating that natural CD4⁺ T_R cells actively engage in negative control of a broad spectrum of immune responses to quasi-self or non-self antigens, as in tumor immunity, organ transplantation, allergy, and microbial immunity (1–3). With *FOXP3* as a useful tool for investigating T_R cells, further characterization of their developmental pathways will facilitate better control of pathologic as well as physiologic immune responses by expansion or reduction of T_R cell populations.

1. Sakaguchi, S. 2000. Regulatory T cells: key controllers of immunologic self-tolerance. *Cell.* **101**:455–458.
2. Shevach, E.M. 2000. Regulatory T cells in autoimmunity. *Annu. Rev. Immunol.* **18**:423–449.
3. Maloy, K.J., and Powrie, F. 2001. Regulatory T cells in the control of immune pathology. *Nat. Immunol.* **2**:816–822.
4. Sakaguchi, S., Sakaguchi, N., Asano, M., Itoh, M., and Toda, M. 1995. Immunologic tolerance maintained by activated T cells expressing IL-2 receptor α-chains (CD25): breakdown of a single mechanism of self-tolerance causes various autoimmune diseases. *J. Immunol.* **155**:1151–1164.
5. Shevach, E.M. 2001. Certified professionals: CD4⁺CD25⁺ suppressor T cells. *J. Exp. Med.* **193**:F41–F46.
6. Gambineri, E., Torgerson, T.R., and Ochs, H.D. 2003. Immune dysregulation, polyendocrinopathy, enteropathy, and X-linked inheritance (IPEX), a syndrome of systemic autoimmunity caused by mutations of FOXP3, a critical regulator of T-cell homeostasis. *Curr. Opin. Rheumatol.* **15**:430–435.
7. Brunkow, M.E., et al. 2001. Disruption of a new forkhead/winged-helix protein, scurfin, results in the fatal lymphoproliferative disorder of the scurfy mouse. *Nat. Genet.* **27**:68–73.
8. Chatila, T.A., et al. 2000. JM2, encoding a fork head-related protein, is mutated in X-linked autoimmunity-allergic disregulation syndrome. *J. Clin. Invest.* **106**:R75–R81.
9. Wildin, R.S., et al. 2001. X-linked neonatal diabetes mellitus, enteropathy and endocrinopathy syndrome is the human equivalent of mouse scurfy. *Nat. Genet.* **27**:18–20.
10. Bennett, C.L., et al. 2001. The immune dysregulation, polyendocrinopathy, enteropathy, X-linked syndrome (IPEX) is caused by mutations of FOXP3. *Nat. Genet.* **27**:20–21.
11. Hori, S., Nomura, T., and Sakaguchi, S. 2003. Control of regulatory T cell development by the transcription factor Foxp3. *Science.* **299**:1057–1061.
12. Fontenot, J.D., Gavin, M.A., and Rudensky, A.Y. 2003. Foxp3 programs the development and function of CD4⁺CD25⁺ regulatory T cells. *Nat. Immunol.* **4**:330–336.
13. Khattri, R., Cox, T., Yasayko, S.A., and Ramsdell, F. 2003. An essential role for Scurfin in CD4⁺CD25⁺ T regulatory cells. *Nat. Immunol.* **4**:337–342.
14. Walker, M.R., et al. 2003. Induction of FoxP3 and acquisition of T regulatory activity by stimulated human CD4⁺CD25⁻ T cells. *J. Clin. Invest.* **112**:1437–1443. doi:10.1172/JCI200319441.
15. Thorstenson, K.M., and Khoruts, A. 2001. Generation of anergic and potentially immunoregulatory CD25⁺CD4 T cells in vivo after induction of peripheral tolerance with intravenous or oral antigen. *J. Immunol.* **167**:188–195.
16. Apostolou, I., Sarukhan, A., Klein, L., and von Boehmer, H. 2002. Origin of regulatory T cells with known specificity for antigen. *Nat. Immunol.* **3**:756–763.
17. Annacker, O., Burlen-Defranoux, O., Pimenta-Araujo, R., Cumano, A., and Bandeira, A. 2000. Regulatory CD4 T cells control the size of the peripheral activated/memory CD4 T cell compartment. *J. Immunol.* **164**:3573–3580.
18. Gavin, M.A., Clarke, S.R., Negrou, E., Gallegos, A., and Rudensky, A. 2002. Homeostasis and anergy

of $CD4^+CD25^+$ suppressor T cells in vivo. *Nat. Immunol.* **3**:33–41.
19. Stephens, L.A., and Mason, D. 2000. CD25 is a marker for $CD4^+$ thymocytes that prevent autoimmune diabetes in rats, but peripheral T cells with this function are found in both $CD25^+$ and $CD25^-$ subpopulations. *J. Immunol.* **165**:3105–3110.
20. Levings, M.K., et al. 2002. Human $CD25^+CD4^+$ T suppressor cell clones produce transforming growth factor beta, but not interleukin 10, and are distinct from type 1 T regulatory cells. *J. Exp. Med.* **196**:1335–1346.
21. O'Garra, A., and Vieira, P., et al. 2003. Twenty-first century Foxp3. *Nat. Immunol.* **4**:304–306.

(Qiagen). Semi-quantitative RT–PCR was performed using a nested protocol as described by ref. 11. Positive control RNA was provided by C. Drosten (Bernhard Nocht Institute for Tropical Medicine, National Reference Center for Tropical Diseases). Virus titration was performed by seeding 5×10^3 Vero E6 cells per well in 96-well microtitre plates 1 day before infection. Culture supernatant from infected 293T cells was added to the first set of wells in triplicate and serially diluted. Cells were monitored for CPE 3 days after infection of Vero E6 cells. The effect of affinity-purified goat anti-ACE1 or -ACE2 antibody on SARS-CoV-induced cytopathicity was measured by reading absorbance at 492 nm of cells incubated with CellTiter 96 (Promega).

Received 14 September; accepted 23 October 2003; doi:10.1038/nature02145.

1. Gallagher, T. M. & Buchmeier, M. J. Coronavirus spike proteins in viral entry and pathogenesis. *Virology* **279**, 371–374 (2001).
2. Holmes, K. V. SARS-associated coronavirus. *N. Engl. J. Med.* **348**, 1948–1951 (2003).
3. Donoghue, M. *et al.* A novel angiotensin-converting enzyme-related carboxypeptidase (ACE2) converts angiotensin I to angiotensin 1–9. *Circ. Res.* **87**, E1–E9 (2000).
4. Tipnis, S. R. *et al.* A human homolog of angiotensin-converting enzyme. Cloning and functional expression as a captopril-insensitive carboxypeptidase. *J. Biol. Chem.* **275**, 33238–33243 (2000).
5. Holmes, K. V. *et al.* Coronavirus receptor specificity. *Adv. Exp. Med. Biol.* **342**, 261–266 (1993).
6. Dveksler, G. S. *et al.* Several members of the mouse carcinoembryonic antigen-related glycoprotein family are functional receptors for the coronavirus mouse hepatitis virus-A59. *J. Virol.* **67**, 1–8 (1993).
7. Delmas, B. *et al.* Aminopeptidase N is a major receptor for the entero-pathogenic coronavirus TGEV. *Nature* **357**, 417–420 (1992).
8. Tresnan, D. B. & Holmes, K. V. Feline aminopeptidase N is a receptor for all group I coronaviruses. *Adv. Exp. Med. Biol.* **440**, 69–75 (1998).
9. Yeager, C. L. *et al.* Human aminopeptidase N is a receptor for human coronavirus 229E. *Nature* **357**, 420–422 (1992).
10. Ksiazek, T. G. *et al.* A novel coronavirus associated with severe acute respiratory syndrome. *N. Engl. J. Med.* **348**, 1953–1966 (2003).
11. Drosten, C. *et al.* Identification of a novel coronavirus in patients with severe acute respiratory syndrome. *N. Engl. J. Med.* **348**, 1967–1976 (2003).
12. Kuiken, T. *et al.* Newly discovered coronavirus as the primary cause of severe acute respiratory syndrome. *Lancet* **362**, 263–270 (2003).
13. Fouchier, R. A. *et al.* Aetiology: Koch's postulates fulfilled for SARS virus. *Nature* **423**, 240 (2003).
14. Rota, P. A. *et al.* Characterization of a novel coronavirus associated with severe acute respiratory syndrome. *Science* **300**, 1394–1399 (2003).
15. Marra, M. A. *et al.* The Genome sequence of the SARS-associated coronavirus. *Science* **300**, 1399–1404 (2003).
16. Sturman, L. S. & Holmes, K. V. Proteolytic cleavage of peplomeric glycoprotein E2 of MHV yields two 90K subunits and activates cell fusion. *Adv. Exp. Med. Biol.* **173**, 25–35 (1984).
17. Jackwood, M. W. *et al.* Spike glycoprotein cleavage recognition site analysis of infectious bronchitis virus. *Avian Dis.* **45**, 366–372 (2001).
18. Spaan, W., Cavanagh, D. & Horzinek, M. C. Coronaviruses: structure and genome expression. *J. Gen. Virol.* **69**, 2939–2952 (1988).
19. Bonavia, A., Zelus, B. D., Wentworth, D. E., Talbot, P. J. & Holmes, K. V. Identification of a receptor-binding domain of the spike glycoprotein of human coronavirus HCoV-229E. *J. Virol.* **77**, 2530–2538 (2003).
20. Breslin, J. J. *et al.* Human coronavirus 229E: receptor binding domain and neutralization by soluble receptor at 37 degrees C. *J. Virol.* **77**, 4435–4438 (2003).
21. Kubo, H., Yamada, Y. K. & Taguchi, F. Localization of neutralizing epitopes and the receptor-binding site within the amino-terminal 330 amino acids of the murine coronavirus spike protein. *J. Virol.* **68**, 5403–5410 (1994).
22. Komatsu, T. *et al.* Molecular cloning, mRNA expression and chromosomal localization of mouse angiotensin-converting enzyme-related carboxypeptidase (mACE2). *DNA Seq.* **13**, 217–220 (2002).
23. Harmer, D., Gilbert, M., Borman, R. & Clark, K. L. Quantitative mRNA expression profiling of ACE 2, a novel homologue of angiotensin converting enzyme. *FEBS Lett.* **532**, 107–110 (2002).
24. Choe, H. *et al.* The beta-chemokine receptors CCR3 and CCR5 facilitate infection by primary HIV-1 isolates. *Cell* **85**, 1135–1148 (1996).
25. Leung, W. K. *et al.* Enteric involvement of severe acute respiratory syndrome-associated coronavirus infection. *Gastroenterology* **125**, 1011–1017 (2003).
26. Crackower, M. A. *et al.* Angiotensin-converting enzyme 2 is an essential regulator of heart function. *Nature* **417**, 822–828 (2002).
27. Vickers, C. *et al.* Hydrolysis of biological peptides by human angiotensin-converting enzyme-related carboxypeptidase. *J. Biol. Chem.* **277**, 14838–14843 (2002).
28. Delmas, B. *et al.* Determinants essential for the transmissible gastroenteritis virus-receptor interaction reside within a domain of aminopeptidase-N that is distinct from the enzymatic site. *J. Virol.* **68**, 5216–5224 (1994).
29. Huang, L. *et al.* Novel peptide inhibitors of angiotensin-converting enzyme 2. *J. Biol. Chem.* **278**, 15532–15540 (2003).
30. Dales, N. A. *et al.* Substrate-based design of the first class of angiotensin-converting enzyme-related carboxypeptidase (ACE2) inhibitors. *J. Am. Chem. Soc.* **124**, 11852–11853 (2002).

Supplementary Information accompanies the paper on **www.nature.com/nature**.

Acknowledgements We thank J. Coderre for assistance with RT–PCR, M. Kirk for editing, and S. H. Wang, E. Kieff, J. Sodroski, C. Gerard and N. Gerard for guidance and helpful conversations.

Competing interests statement The authors declare that they have no competing financial interests.

Correspondence and requests for materials should be addressed to H.C. (hyeryun.choe@tch.harvard.edu) or M.F. (farzan@mbcrr.harvard.edu).

Altered thymic T-cell selection due to a mutation of the ZAP-70 gene causes autoimmune arthritis in mice

Noriko Sakaguchi[1,2]*, Takeshi Takahashi[1]*, Hiroshi Hata[1], Takashi Nomura[1], Tomoyuki Tagami[1], Sayuri Yamazaki[1], Toshiko Sakihama[1], Takaji Matsutani[3], Izumi Negishi[4], Syuichi Nakatsuru[1] & Shimon Sakaguchi[1,2]

[1]*Department of Experimental Pathology, Institute for Frontier Medical Sciences, Kyoto University, Kyoto 606-8507, Japan*
[2]*Laboratory for Immunopathology, RIKEN Research Center for Allergy and Immunology, Yokohama 230-0045, Japan*
[3]*Department of Immunology, Shionogi Institute for Medical Science, Settsu, Osaka 566-0022, Japan*
[4]*Department of Dermatology, Gunma University Hospital, Maebashi, Gunma 371-8511, Japan*

* These authors contributed equally to this work

Rheumatoid arthritis (RA), which afflicts about 1% of the world population, is a chronic systemic inflammatory disease of unknown aetiology that primarily affects the synovial membranes of multiple joints[1–3]. Although $CD4^+$ T cells seem to be the prime mediators of RA, it remains unclear how arthritogenic $CD4^+$ T cells are generated and activated[1–3]. Given that highly self-reactive T-cell clones are deleted during normal T-cell development in the thymus, abnormality in T-cell selection has been suspected as one cause of autoimmune disease[4,5]. Here we show that a spontaneous point mutation of the gene encoding an SH2 domain of ZAP-70, a key signal transduction molecule in T cells[6], causes chronic autoimmune arthritis in mice that resembles human RA in many aspects. Altered signal transduction from T-cell antigen receptor through the aberrant ZAP-70 changes the thresholds of T cells to thymic selection, leading to the positive selection of otherwise negatively selected autoimmune T cells. Thymic production of arthritogenic T cells due to a genetically determined selection shift of the T-cell repertoire towards high self-reactivity might also be crucial to the development of disease in a subset of patients with RA.

The SKG strain, which spontaneously develops chronic arthritis, is derived from our closed breeding colony of BALB/c mice. Joint swelling with hyperaemia became macroscopically evident in SKG mice at about 2 months of age, initially at a few interphalangeal joints of the forepaws, then progressing in a symmetrical fashion to swelling of other finger joints of the forepaws and hindpaws, and larger joints (wrists and ankles) (Fig. 1a–d). Knee, elbow, shoulder or vertebral joints were rarely affected except for the joint at the base of the tail in aged SKG mice (Fig. 1e). Radiographic examination revealed destruction and fusion of the subchondral bones, joint dislocation, and osteoporosis by 8–12 months of age (Fig. 1f–i). Despite suffering from such severe chronic arthritis, most SKG mice survived well to 1 year of age, generally with more severe arthritides in females (Fig. 1j).

Histology of the swollen joints showed severe synovitis with massive subsynovial infiltration of neutrophils, lymphocytes, macrophages and plasma cells, villus proliferation of synoviocytes accompanying pannus formation and neovascularization, and neutrophil-rich exudates in the joint cavity (Fig. 1k, l), with progression of synoviocyte proliferation, pannus-eroded adjacent cartilage and subchondral bone. Immunohistochemical staining revealed that $CD4^+$ T cells predominantly infiltrated the subsynovial tissue (Fig. 1m, n). As extra-articular manifestations of the disease, most (more than 90%) mice older than 6 months of age developed interstitial pneumonitis with various degrees of perivascular and

peribronchiolar cellular infiltration (Fig. 1o); more than 90% showed infiltration of inflammatory cells in the skin (Supplementary Fig. 1a). Some (10–20%) mice had subcutaneous necrobiotic nodules, not unlike rheumatoid nodules in RA (Fig. 1p), and vasculitides (Supplementary Fig. 1b). SKG mice did not show lymphoadenopathy or lupus-like diseases (such as immune-complex glomerulonephritis).

SKG mice developed high titres of rheumatoid factor (RF), autoantibodies specific for type II collagen, antibodies reactive with heat shock protein (HSP)-70 of *Mycobacterium tuberculosis* presumably due to a cross-reaction with a conserved epitope of HSP, severe hypergammaglobulinaemia and a high concentration of the circulating immune complexes. However, there were no significant titres of anti-DNA antibodies or organ-specific autoantibodies such as those specific for thyroglobulins or gastric parietal cells[1–3,7] (Fig. 1q–v).

Thus, this spontaneous arthritis in SKG mice resembles RA in clinical and histological characteristics of articular and extra-articular lesions and in serological features[1–3].

Transfer of spleen and lymph node T cells, $CD4^+$ T cells in particular, from arthritic SKG mice produced similar arthritis in

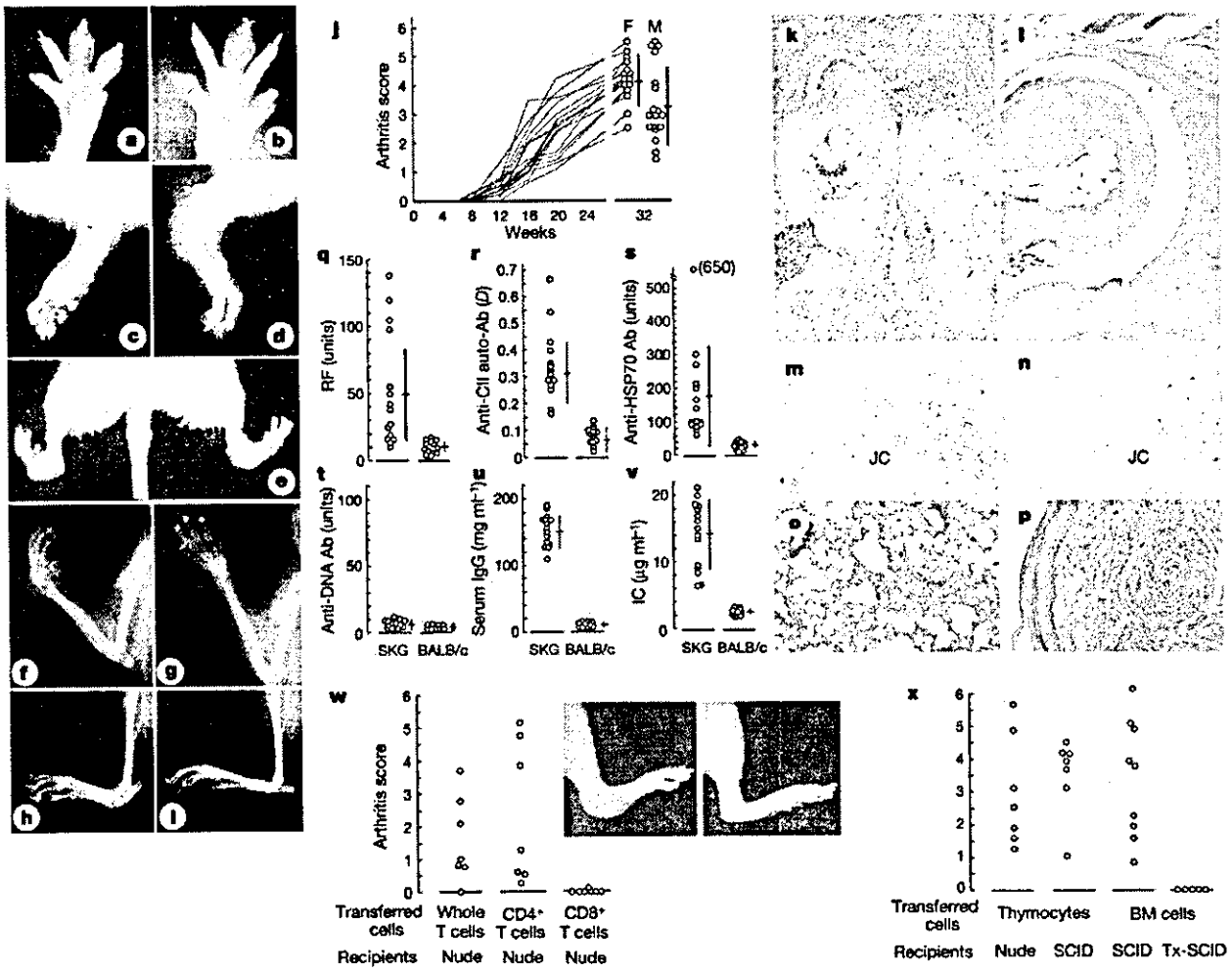

Figure 1 Arthritis in SKG mice. **a–e**, Swelling of joints: fingers (**a**) and toes (**b**) of a 4-month-old SKG mouse; forepaw (**c**) and hindpaw (**d**) of a 6-month-old SKG mouse; deformity of bilateral ankles and swelling of the base of the tail (**e**) in an 18-month-old SKG mouse. **f–i**, X-ray photographs of joints: wrist (**f**) and ankle (**h**) of an 8-month-old SKG mouse, and wrist (**g**) and ankle (**i**) of an 8-month-old BALB/c mouse. **j**, Time course of joint swelling in female SKG mice, and arthritis scores of 8-month-old female (F) and male (M) SKG mice ($n = 15$ each). Vertical bars represent s.e.m. See Methods for details on the scoring of joint swelling. **k–p**, Histology of arthritis and extra-articular lesions in SKG mice: a finger joint of a 6-month-old SKG (**k**) or BALB/c mouse (**l**) (haematoxylin/eosin (HE) staining, original magnification ×40); immunoperoxidase staining of synovial tissue in a finger joint of a 3-month-old SKG mouse with anti-CD4 mAb (GK1.5) (**m**) or anti-CD8 mAb (3–155) (**n**) (magnification ×40) (JC, joint cavity); interstitial pneumonitis (**o**) and a rheumatoid nodule-like lesion (**p**) in an 8-month-old SKG mouse (HE staining, magnification ×40). **q–v**, Serological characteristics of SKG mice: RF (**q**), anti-CII Ab (**r**), anti-HSP70 antibody (Ab) (**s**), anti-DNA antibody (**t**), concentration of IgG (**u**) and immune complexes (**v**) in the sera from 6-month-old female SKG or BALB/c mice ($n = 15$ each). **w**, Adoptive transfer of arthritis. The same dose (2.5×10^7) of whole, $CD4^+$ or $CD8^+$ T cells prepared from lymph nodes and spleens of arthritis-bearing 6-month-old SKG mice were transferred to 6-week-old BALB/c nude mice (SLC, Shizuoka). Inset, swelling of a hindpaw (left) and an intact paw (right) of a nude mouse transferred with $CD4^+$ T cells and with $CD8^+$ T cells, respectively. **x**, Thymocytes (10^8) or T-cell-depleted bone marrow cell suspensions (5×10^6) from the same SKG mice were transferred to 6-week-old nude or C.B.-17 SCID mice (Clea, Tokyo) or SCID mice that had been thymectomized 1 week after birth (Tx-SCID). The severity of arthritis in these mice was assessed 3 months later. $CD4^+$ or $CD8^+$ T cells were prepared by MACS (Miltenyi Biotec) with more than 95% purity. Bone marrow cells were treated with anti-Thy-1, anti-CD4 and anti-CD8 antibody and rabbit complement before transfer[19].

T-cell-deficient athymic BALB/c nude mice (Fig. 1w), whereas transfer of the sera from the same SKG mice did not (data not shown). Transfer of thymocyte suspensions from arthritic or non-arthritic young SKG mice also elicited severe arthritis in BALB/c nude mice and T/B-cell-deficient C.B-17 severe combined immunodeficiency (SCID) mice (Fig. 1x), whereas thymocyte transfer from normal BALB/c mice did not[8]. Furthermore, transfer of T-cell-depleted bone marrow cell suspensions from SKG mice produced severe arthritis in SCID mice, but not in SCID mice thymectomized before the transfer (Fig. 1x). These results collectively indicate that, first, the RA-like arthritis in SKG mice is a genuine autoimmune disease mediated by apparently joint-specific $CD4^+$ T cells; second, the SKG thymus is continuously generating arthritogenic autoimmune T cells; and, third, the SKG bone marrow cells give rise to such arthritogenic T cells through the normal thymic environment, indicating that the arthritogenic abnormality in SKG mice is intrinsic to T cells.

The primary cause of the arthritis in SKG mice is a genetic abnormality, not vertical or horizontal transmission of arthritogenic microbes. The offspring of crosses between SKG and normal BALB/c mice, whether the mother was SKG or BALB/c, developed no arthritis (Fig. 2a). In contrast, arthritis with a clinical course and severity similar to that in SKG mice occurred in about 50% of the N_2 generation obtained by crossing the non-arthritic F_1 hybrids with SKG. Thus, the genetic abnormality was presumably of a single gene locus (designated the *skg* gene) and inherited in an autosomal recessive fashion with nearly 100% penetrance of the trait in homozygotes raised in our conventional environment.

Linkage analysis between the development of macroscopically evident arthritis and the homozygosity of chromosome-specific microsatellite markers, performed by using the N_2 generation with *Mus musculus castaneus* (CAST/Ei) (that is, SKG × (SKG × CAST/Ei)F_1 mice), mapped the *skg* locus to the centromeric portion of chromosome 1 with the lod score of the locus as infinite (Fig. 2b). Another significant linkage was with the region around the *H-2* locus on chromosome 17 (Fig. 2c). This linkage was observed only when the mice were maintained in a nearly specific-pathogen-free (SPF) condition, but not in arthritis-prone non-SPF conventional

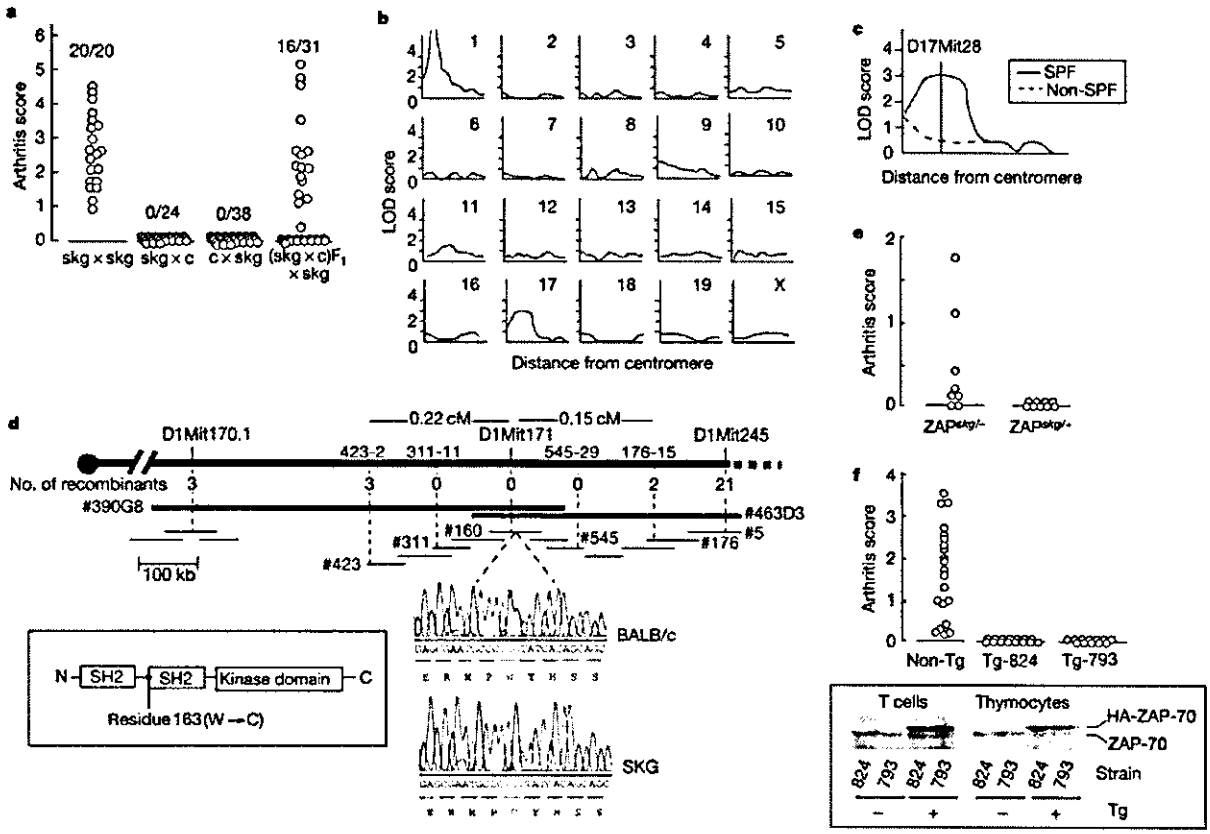

Figure 2 Genetic study of SKG arthritis. **a**, Autosomal recessive inheritance of SKG arthritis. skg × skg, F_1 of mating SKG females with SKG males; skg × c and c × skg, F_1 of mating SKG females with BALB/c males, and BALB/c females with SKG males, respectively; (skg × c)F_1 × skg, N_2 mice of backcrossing (SKG × BALB/c)F_1 mice with SKG mice. **b**, Genome-wide mapping of the *skg* locus. The LOD score curves were obtained by genotyping 58 arthritis-bearing N_2 mice by detecting microsatellite markers (Mouse MapPairs) locating every ~10 cM interval on each chromosome, in accordance with the manufacturer's instruction (Research Genetics). Chromosomes are identified with a number or X in each panel. **c**, Contribution of the loci on chromosome 17 to genetic susceptibility to SKG arthritis in a SPF condition. **d**, Genetic map of the *skg* locus on chromosome 1 with the number of recombinants and physical map of the locus with YAC and BAC clones. Inset shows the structure of the ZAP-70 protein and the position of the *skg* mutation. The ZAP-70^{W163C} mutation in SKG mice was not found in other mouse strains including C57BL/6, C3H, DBA/1, DBA/2, 129$^+$Ter/SV, FvB/N, NOD, MRL-lpr, NZW and CAST/Ei. **e**, SKG mice were mated with heterozygotes of ZAP-70-deficient mice, and the resulting ZAP-$70^{skg/-}$ or ZAP-$70^{skg/+}$ mice were assessed for joint swelling at 5 months of age. **f**, Rescue of SKG arthritis by expressing human normal ZAP-70 transgene[9]. The arthritis score of Tg-824 or Tg-793 mice, which were backcrossed three times to SKG mice, was assessed at 8 months of age. The expression of transgene-derived human ZAP-70 protein with HA-tag was assessed by western blotting with antibody against human ZAP-70 (Santa Cruz Biotech).

condition (lod scores at the D17Mit28 locus: 2.95 in SPF compared with 0.40 in non-SPF). In the former condition, homozygosity of the H-2^d haplotype conferred higher genetic susceptibility to the arthritis, indicating that a polymorphism of the major histocompatibility complex (MHC) gene or the gene(s) linked to it can contribute to determining the susceptibility depending on the environmental conditions.

To identify the *skg* gene, we then constructed a high-resolution genetic map of the *skg* region by using 1,352 mice with arthritis among a total of 2,939 N_2 mice (Fig. 2d). The mapping localized the *skg* locus to a 0.37-cM interval between two simple sequence-length polymorphism markers (nos 176-15 and 423-2), covered by two yeast artificial chromosomes (YACs) and ten bacterial artificial chromosomes (BACs) (Fig. 2d, top). Sequencing of several of these BACs localized the ZAP-70 gene on BAC no. 160. Sequencing of the entire coding region of ZAP-70 cDNA from SKG mice and comparison of the sequence with that of BALB/c mice revealed a homozygous G-to-T substitution at nucleotide 489 in the SKG ZAP-70 gene, which altered codon 163 from tryptophan to cysteine (W163C) (Fig. 2d, bottom). This nucleotide substitution existed in the genomic DNA of SKG mice but not in other strains (see legend to Fig. 2). The position of the mutation corresponds to the initial amino-acid residue of the carboxy-terminal SH2 (SH2C) domain of ZAP-70 (Fig. 2d, inset).

To confirm that the ZAP-70^{W163C} mutation was primarily responsible for SKG arthritis, we crossed SKG mice, which had a ZAP-$70^{skg/skg}$ genotype, with the heterozygotes of ZAP-70-deficient mice (ZAP-$70^{+/-}$) to produce mice with a ZAP-$70^{skg/+}$ or ZAP-$70^{skg/-}$ genotype[9] and assessed the development of arthritis in these mice (Fig. 2e). Most of the ZAP-$70^{skg/-}$ mice developed arthritis spontaneously by 3 months of age, in contrast with no arthritis in the ZAP-$70^{skg/+}$ mice. Other immunological abnormalities of T cells and thymocytes were also similar between SKG mice and ZAP-$70^{skg/-}$ mice but these were corrected in ZAP-$70^{skg/+}$ mice (Supplementary Fig. 2a, and see below). Furthermore, transgenic (Tg) expression of the normal human ZAP-70 gene in SKG mice

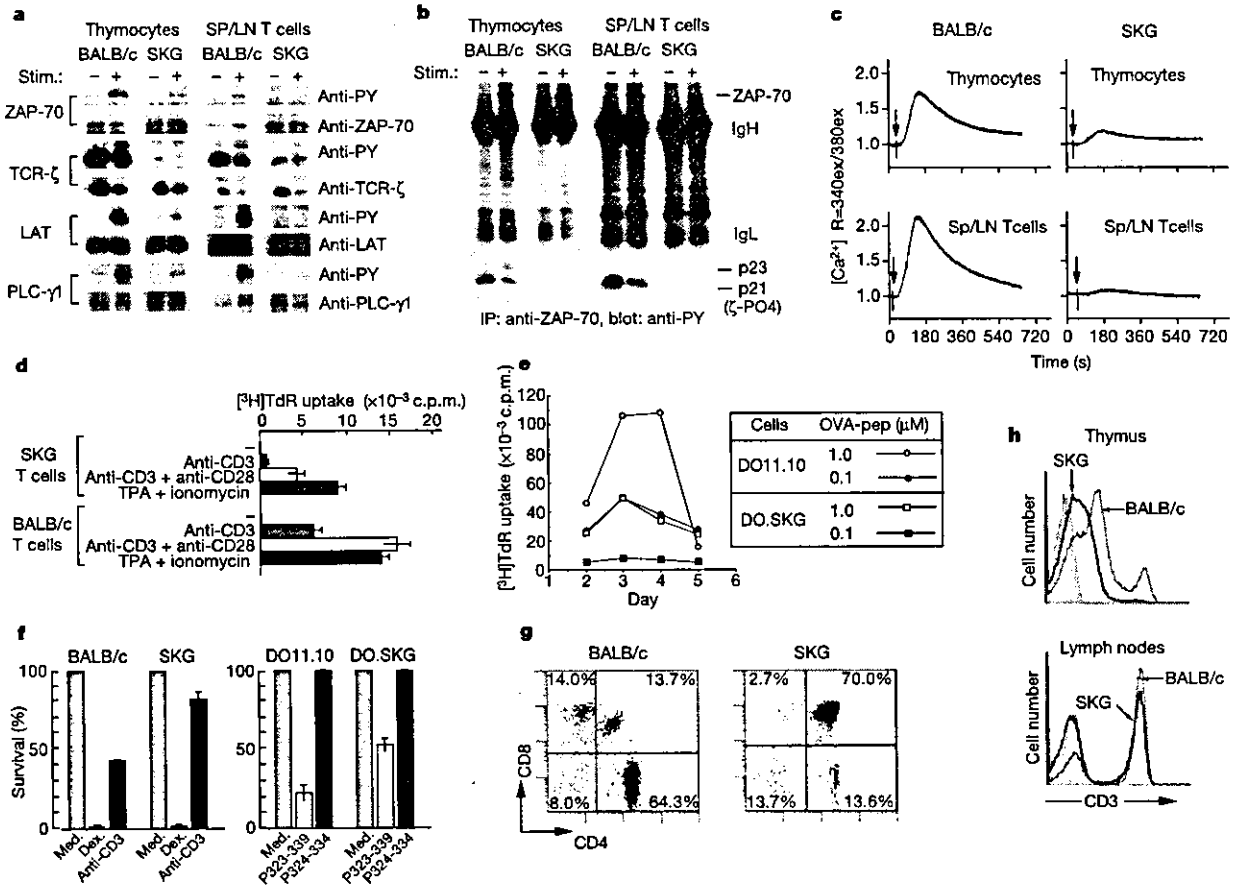

Figure 3 T-cell abnormalities in SKG mice. **a**, Impaired TCR signal transduction in SKG mice. Tyrosine phosphorylation status was assessed by immunoprecipitation and western blotting for ZAP-70, TCR-ζ, LAT and PLC-γ after anti-CD3 mAb stimulation of SKG or BALB/c thymocytes or spleen and lymph node (SP/LN) T cells. **b**, Association between ZAP-70 and TCR-ζ after CD3 crosslinking in SKG T cells and thymocytes. IP, immunoprecipitation. **c**, Ca^{2+} mobilization in SKG T cells or thymocytes after TCR stimulation. **d**, Proliferative responses of SKG T cells to various T-cell stimulations. **e**, Proliferation of $CD4^+$ T cells from DO11.10 or DO.SKG mice stimulated with the indicated concentrations of ovalbumin (OVA) peptides in the presence of BALB/c antigen-presenting cells. **f**, Apoptosis of SKG or BALB/c thymocytes cultured with medium alone (med.), anti-CD3 mAb (2C11, 1 μg ml^{-1}) or dexamethasone (Dex.) (100 nM) (left); apoptosis of DO11.10 or DO.SKG thymocytes cultured with medium alone or indicated ovalbumin peptides (1 μM) (right), as described previously[9]. **g**, Apoptosis of thymocytes in SKG or BALB/c mice injected intraperitoneally with anti-CD3 mAb (2C11; 250 μg) 3 days previously[9]. These figures represent three independent experiments. **h**, Staining of thymocytes or lymph-node cells from a 2-month-old SKG or BALB/c mouse with anti-CD3 mAb.

under the *lck* proximal promoter, which resulted in specific expression of the Tg ZAP-70 protein in thymocytes and peripheral T cells in two Tg lines, completely inhibited the development of arthritis and corrected other immunological abnormalities, contrasting with 100% incidence of arthritis in non-Tg littermates (Fig. 2f and Supplementary Fig. 2b).

Taken together, these results indicate that the ZAP-70^{W163C} alteration is not a mere polymorphism but is the causative mutation of SKG arthritis.

To determine, then, how the ZAP-70 mutation affects T-cell signal transduction, we assessed thymocytes and T cells from SKG or BALB/c mice for the tyrosine-phosphorylation status of major signal transduction molecules, including ZAP-70, TCR-ζ, LAT and PLC-γ1 (refs 6, 10–12; Fig. 3a, b). After stimulation with anti-CD3 monoclonal antibody (mAb), the levels of phosphorylation of these molecules were extremely low in SKG thymocytes and T cells. Calcium mobilization, one of the earliest events induced by TCR stimulation, was also greatly impaired in SKG thymocytes and T cells, presumably because of the decreased phosphorylation of PLC-γ1 (Fig. 3c). Immunoprecipitation of ZAP-70 from stimulated SKG thymocytes or T cells failed to co-precipitate tyrosine-phosphorylated p21 and p23 isoforms of TCR-ζ, indicating defective interactions between ZAP-70 and TCR-ζ[10,11] (Fig. 3b). Furthermore, downstream mitogen-activated protein (MAP) kinase signalling pathways involving ERK, JNK and p38 MAP kinases were also attenuated in SKG thymocytes[13] (Supplementary Fig. 3). SKG T cells showed no enhancement of the expression of Syk, another protein tyrosine kinase that might compensate for the role of ZAP-70 in T cells[14] (T.T., unpublished data). These results collectively indicate that the ZAP-70^{W163C} mutation might impair the recruitment and association of ZAP-70 to tyrosine-phosphorylated immunoreceptor tyrosine-based activation motifs (ITAMs) of TCR-ζ and CD3 chains, thereby altering signal transduction through ZAP-70.

In accord with this attenuated signal transduction through ZAP-70, SKG T cells were hyporesponsive to polyclonal TCR stimulation *in vitro*, for example with anti-CD3 mAb, whereas they responded well to stimulation by 12-*O*-tetradecanoylphorbol-13-acetate (TPA) and ionomycin, which transduces a signal to TCR-distal pathways (Fig. 3d). When the *skg* gene was homozygously introduced to DO11.10 TCR-Tg mice, in which most T cells express Tg TCRs specific for an ovalbumin peptide[15], T cells from such mice (designated DO.SKG mice) required a peptide concentration 10-fold that in DO11.10 T cells to exhibit an equivalent magnitude of proliferation (Fig. 3e). Furthermore, SKG thymocytes were resistant to apoptosis induced by TCR stimulation, but not to dexamethasone-induced apoptosis, as shown by the stimulation of SKG or DO.SKG thymocytes *in vitro* with anti-CD3 mAb or the specific peptide, respectively (Fig. 3f), or by inoculation with anti-CD3 mAb *in vivo* (Fig. 3g).

SKG mice were also aberrant in T-cell development. In comparison with normal BALB/c mice, TCR^{high} mature thymocytes decreased in number and ratio, whereas TCR^{low} immature thymocytes increased in the SKG thymus; the levels of TCR expression on

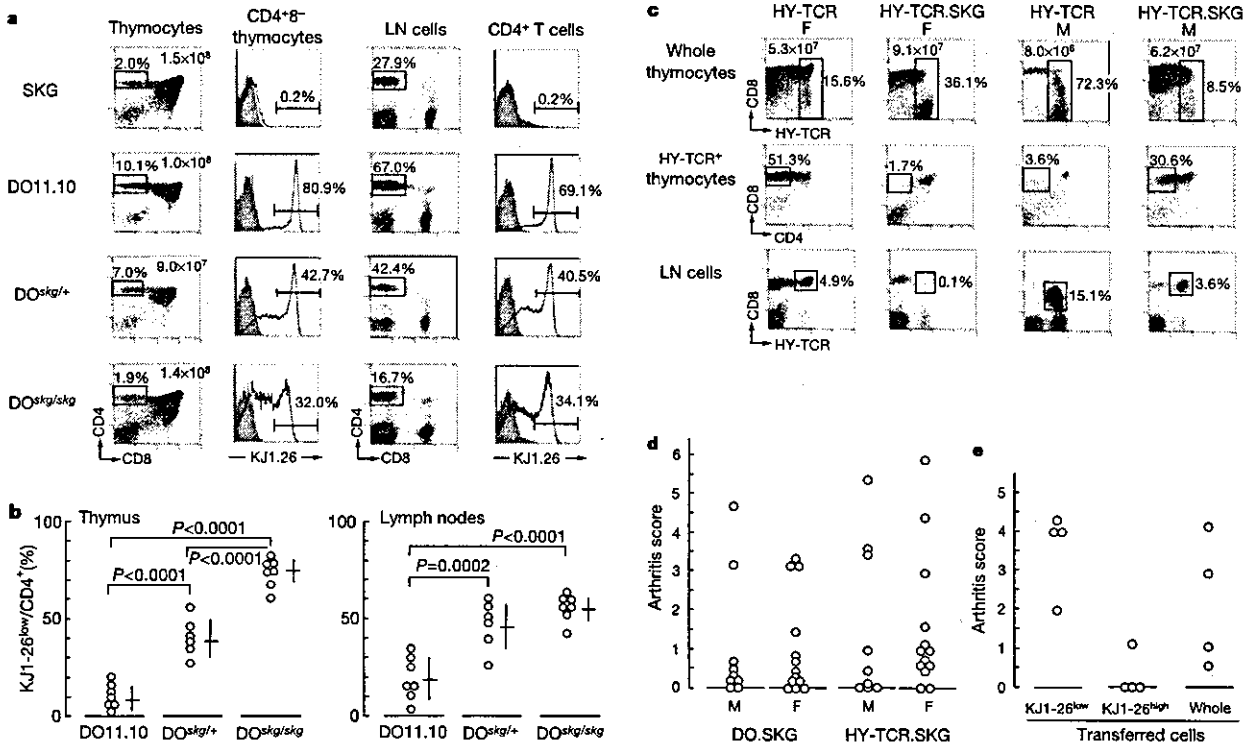

Figure 4 Altered thymic T-cell selection in SKG mice. **a**, Staining of thymocytes or lymph-node cells from a 4-month-old DO11.10, DO$^{skg/skg}$ or DO$^{skg/+}$ mouse with the indicated monoclonal antibodies. Dot-plot figures are scaled logarithmically. Ordinates of histograms denote cell number (arbitrary units). **b**, The percentage of KJ1-26^{low} T cells among CD4$^+$CD8$^-$ thymocytes or CD4$^+$ T cells was also assessed for individual DO11.10, DO$^{skg/+}$ or DO$^{skg/skg}$ mice. **c**, Staining of thymocytes or lymph-node cells from a 4-month-old female or male HY-TCR or HY-TCR.SKG transgenic mouse with the indicated monoclonal antibodies. **d**, Arthritis scores of 6-month-old DO.SKG or HY-TCR.SKG mice. **e**, Adoptive transfer of arthritis from arthritis-bearing DO.SKG mice to SCID mice, which were assessed for joint swelling 2 months later. Each fraction of cells (10^6) was purified by cell sorter from CD4$^+$ lymph node and spleen cells.

mature thymocytes or peripheral T cells were comparable between the two strains (Fig. 3h). The numbers of peripheral $CD4^+$ and $CD8^+$ T cells consequently decreased in SKG mice, with a relative increase in B cells (Supplementary Fig. 4). There was no significant difference in the total number of thymocytes or spleen cells, the thymic architecture, the number and function of natural killer cells (which express ZAP-70) or the composition of T-cell subpopulations expressing particular TCR Vα or Vβ families (Supplementary Fig. 5).

We then assessed the effects of the *skg* mutation on thymic positive and negative selection by introducing the *skg* gene homozygously into TCR-Tg mice[15,16]. In DO.SKG (that is, $DO^{skg/skg}$) mice, the number of $CD4^+CD8^-$ mature thymocytes decreased to ~20% of normal DO11.10 mice (Fig. 4a). Furthermore, only ~30% of $CD4^+CD8^-$ thymocytes were Tg-TCR^{high} (when stained with clonotype-specific KJ1-26 mAb)[15] in contrast to ~80% in DO11.10 mice (Fig. 4a, b); the rest of $CD4^+CD8^-$ thymocytes (that is, KJ1-26^{low}, hence Tg-TCR^{low} thymocytes) in $DO^{skg/skg}$ mice seemed to express endogenous TCR α-chains. Similarly, Tg-TCR^{high} T cells constituted only ~30% of $CD4^+$ T cells in the periphery of $DO^{skg/skg}$ mice, contrasting with ~70% in DO11.10 mice (Fig. 4a, b); Tg-TCR^{low} T cells in $DO^{skg/skg}$ mice expressed endogenous α-chains associated with transgenic β-chains (Supplementary Fig. 6). In *skg*-heterozygous $DO^{skg/+}$ mice, the decrease or increase in the percentage of Tg-TCR^{high} or Tg-TCR^{low} T cells, respectively, in the thymus and the periphery was intermediate between that in the $DO^{skg/skg}$ and that in DO11.10 mice (Fig. 4a, b).

In HY-TCR Tg mice that express transgenic TCRs specific for male-specific HY antigens on an $H\text{-}2^b$ background, female HY-TCR Tg mice positively selected HY-$TCR^+CD8^+CD4^-$ thymocytes (detected by clonotype-specific T3.70 mAb)[16]. In contrast, female HY-TCR Tg mice with the homozygous *skg* gene (designated HY-TCR.SKG Tg mice) on an $H\text{-}2^b$ background hardly showed any positive selection of HY-$TCR^+CD8^+CD4^-$ thymocytes and T cells[17] (Fig. 4c). However, in contrast to substantial deletion of HY-$TCR^+CD8^+CD4^-$ thymocytes in male HY-TCR Tg mice, male HY-TCR.SKG Tg mice showed efficient positive selection of HY-$TCR^+CD8^+CD4^-$ thymocytes in almost a comparable number to those in female HY-TCR Tg mice. Furthermore, HY-TCR^+ peripheral T cells in male HY-TCR.SKG Tg mice expressed nearly normal levels of CD8 expression, contrasting with low-level CD8 expression in male HY-TCR Tg mice[16].

Both DO.SKG and HY-TCR.SKG mice developed arthritis at high incidences (Fig. 4d). Transfer of Tg-TCR^{low} cells (as KJ1-26^{low} cells) from such arthritis-bearing DO.SKG mice to C.B-17 SCID mice induced arthritis, whereas transfer of Tg-TCR^{high} cells did not (Fig. 4e), indicating that TCR-Tg mice with the *skg* mutation positively select arthritogenic T cells expressing endogenous TCR α-chains paired with transgenic β-chains (see above).

Taken together, these results show that the *skg* mutation alters the sensitivity of developing thymocytes to both positive and negative selection, thereby leading to positive selection of otherwise negatively selected autoimmune T cells. This recessive mutation affects T-cell selection even in the heterozygotes, although to a smaller degree than in the homozygotes. Furthermore, the degree of impairment in T-cell signal transduction through ZAP-70 can determine the degree of thymic positive or negative selection, and consequently the phenotype of immunological diseases. The *skg* mutation of the SH2C domain of ZAP-70 elicits autoimmune arthritis, whereas a mutation in the kinase domain of ZAP-70 leads to a severe impairment of positive selection and hence total T-cell deficiency[18].

On the assumption that thymic positive and negative selection of developing T cells requires a certain range of TCR signal through ZAP-70, the *skg* mutation is likely to raise the threshold of TCR avidity for self-peptide/MHC ligands required for the selection to compensate for the reduced signal through the aberrant ZAP-70. This results in a 'selection shift' of the T-cell repertoire towards high reactivity to self-peptide/MHC ligands in the thymus, leading to the thymic production of highly self-reactive T cells that would not be produced by the normal thymuses of ZAP-70-intact animals. The pathogenic self-reactive T cells thus produced by the SKG thymus apparently overcome the mechanisms of peripheral self-tolerance, for example, mediated by naturally occurring $CD25^+CD4^+$ regulatory T cells[8,19]. However, it remains to be determined whether the *skg* mutation might also alter the repertoire of $CD25^+CD4^+$ regulatory T cells or somehow affect their suppressive activity[8,19].

A critical question on SKG arthritis is why this general alteration in T-cell repertoire should lead to the predominant development of autoimmune arthritis but not other autoimmune diseases. In contrast with other organ-specific autoimmune diseases in which self-reactive T cells destroy the target cells (for example, type 1 diabetes due to destruction of insulin-secreting pancreatic β-cells), a cardinal feature of autoimmune arthritis in SKG mice (and also RA in humans) is that self-reactive T cells do not destroy synoviocytes but stimulate them to proliferate[1–3]. This is partly due to a high sensitivity of synoviocytes to various stimuli that can activate them (as also illustrated by other arthritis models[7,19–25]) and their distinct capacity to secrete proinflammatory cytokines (such as interleukin-1, interleukin-6 and tumour necrosis factor-α) and chemical mediators that destroy the surrounding cartilage and bone[1–3,26,27]. It is therefore likely that this unique combination of a high and broad self-reactivity of SKG T cells and a high susceptibility of synovial cells to inflammatory stimuli (including T-cell self-reactivity) leads to predominant development of autoimmune arthritis in SKG mice.

Our findings indicate that mutations of other loci of the ZAP-70 gene or the genes encoding other signalling molecules especially at TCR proximal steps, even if they are heterozygous mutations, might contribute to the development of autoimmune disease by affecting thymic T-cell selection[28–30]. Indeed, we have recently found heterozygous mutations in the ITAM regions of the TCR-ζ chain gene in 2.5% of 160 RA patients in our hospital (H.H., N.S., S.N., T.N. and S.S., unpublished observations). Physical association between these mutated TCR-ζ chain molecules and the normal ZAP-70 molecules, assessed by surface plasmon resonance, was significantly lower than normal as observed between the mutated ZAP-70 in SKG mice and the normal TCR-ζ chain (T.N. and S.S., unpublished data). As RA is a heterogeneous disease with complex genetics[1–3], RA with a similar aetiology to SKG arthritis represents only a fraction of the disease. Nevertheless, further analyses of SKG arthritis at each step of the pathogenetic pathway from the ZAP-70 mutation, through thymic generation of autoimmune T cells, to the activation of arthritogenic T cells and inflammatory destruction of the joint, will explain how genetic and environmental factors contribute to the development of RA. This will help in the design of effective methods of detection, treatment and prevention of RA. □

Methods

Scoring of joint swelling

Joint swelling was monitored by inspection and scored as follows: 0, no joint swelling; 0.1, swelling of one finger joint; 0.5, mild swelling of wrist or ankle; 1.0, severe swelling of wrist or ankle. Scores for all fingers of forepaws and hindpaws, wrists and ankles were totalled for each mouse.

Enzyme-linked immunosorbent assay (ELISA)

Affinity-purified mouse IgG (5 μg ml^{-1}), 10 μg ml^{-1} bovine type II collagen (Funakoshi), 5 μg ml^{-1} double or single-stranded-DNA, or 10 μg ml^{-1} HSP-70 of *Mycobacterium tuberculosis* in PBS, pH 7.2, were used for overnight coating of ELISA plates (Flow Laboratories)[7,8]. Test sera were diluted 1:10 for anti-type II collagen or anti-HSP-70 assay, 1:20 for RF assay, or 1:40 for anti-DNA assay. Alkaline-phosphatase-conjugated anti-mouse IgG or IgM (for RF assay) (Southern Biotechnology Associates) was used at 1 μg ml^{-1} as the secondary reagent[7,8]. Pooled serum from MRL-lpr mice was used as the standard of arbitrary units in the RF, anti-DNA or anti-HSP70 antibody assay[7]. The titre of anti-CII antibody was expressed as attenuance. The amount of immune complex was measured by anti-C3 assay; the serum concentration of IgG was measured by the single radial immunodiffusion method[7].

In vitro T-cell activation

SKG or BALB/c T cells (3.0×10^4) were stimulated for 72 h with plate-bound anti-CD3 mAb (2C11) in the presence or absence of plate-bound anti-CD28 mAb in RPMI-1640 medium supplemented with 10% fetal calf serum and 50 μM 2-mercaptoethanol. Cells were also stimulated with TPA (1.4 ng ml^{-1}) and ionomycin (0.14 μM). KJ1.26$^+$ T cells from DO or DO.SKG mice were stimulated with ovalbumin (323–339) peptide in the presence of X-irradiated syngeneic spleen cells (10^5 cells) as antigen-presenting cells in 96-well round-bottomed plates. The incorporation of [^{3}H]thymidine by proliferating lymphocytes during the last 6 h of the culture was measured.

Immunoprecipitation and western blotting

Thymocytes or purified T cells (5×10^6) were incubated with anti-CD3 mAb (2C11) for 20 min, followed by cross-linking with antibody against Armenian hamster immunoglobulin (Jackson ImmunoResearch) (10 μg ml^{-1}) at 37 °C for the indicated duration. For immunoprecipitation, cells were lysed with RIPA buffer (0.5% Triton X-100, 20 mM Tris-HCl pH 7.5, 1 mM EDTA, 150 mM NaCl, 20 mM NaF, 1 mM Na_3VO_4) supplemented with protease inhibitors. The immune complexes were recovered by Protein A-conjugated Sepharose beads. For western blot analyses, cells were directly lysed by sample-loading buffer for SDS–polyacrylamide gel electrophoresis (SDS–PAGE) and immediately boiled for 4 min. Recovered immune complexes or total cell lysates were subjected to SDS–PAGE and transferred to poly(vinylidene difluoride) membranes, which were blotted with various antibodies after being blocked with PBS/5% BSA. Antibodies specific for the following proteins were used: ZAP-70 (Santa Cruz Biotech), TCR-ζ (Santa Cruz Biotech), LAT (Upstate Biotechnology), PLC-γ1 (Upstate Biotechnology), activated or total ERK1/2, SAPK/JNK and p38 MAP kinases (Cell Signalling Technology) or phosophotyrosine (4G10) (Upstate Biotechnology).

Calcium mobilization

Thymocytes or purified T cells were loaded with Fura-2 acetoxymethyl ester (Nacarai) for 30 min at 37 °C. Cells were then incubated with anti-CD3 mAb as described above, washed and resuspended with PBS. $CaCl_2$ was added to the samples 2 min before cross-linking cell surface-bound anti-CD3 mAb with anti-hamster antibody (Jackson ImmunoResearch). Fura-2 fluorescence was measured by a spectrofluorimeter (Nihon Bunkou).

Received 4 August; accepted 13 October 2003; doi:10.1038/nature02119.

1. Harris, E. D. *Rheumatoid Arthritis* (W. B. Saunders, Philadelphia, 1997).
2. Feldmann, M., Brennan, F. M. & Maini, R. N. Rheumatoid arthritis. *Cell* **85**, 307–310 (1996).
3. Firestein, G. F. in *Textbook of Rheumatology* 5th edn (eds Kelley, W. N., Ruddy, S., Harris, E. D. & Sledge, C. B.) 851–897 (W. B. Saunders, Philadelphia, 1997).
4. Marrack, P., Kappler, J. & Kotzin, B. L. Autoimmune disease: why and where it occurs. *Nature Med.* **7**, 899–905 (2001).
5. von Boehmer, H. *et al.* Thymic selection revisited: how essential is it? *Immunol. Rev.* **191**, 62–78 (2003).
6. Chan, A. C., Iwashima, M., Turck, C. W. & Weiss, A. ZAP-70: a 70 kd protein-tyrosine kinase that associates with the TCR zeta chain. *Cell* **71**, 649–662 (1992).
7. Sakaguchi, S. & Sakaguchi, N. Thymus and autoimmunity: capacity of the normal thymus to produce pathogenic self-reactive T cells and conditions required for their induction of autoimmune disease. *J. Exp. Med.* **172**, 537–545 (1990).
8. Itoh, M. *et al.* Thymus and autoimmunity: production of CD25$^+$ CD4$^+$ naturally anergic and suppressive T cells as a key function of the thymus in maintaining immunologic self-tolerance. *J. Immunol.* **162**, 5317–5326 (1999).
9. Negishi, I. *et al.* Essential role for ZAP-70 in both positive and negative selection of thymocytes. *Nature* **376**, 435–438 (1995).
10. van Oers, N. S. *et al.* The 21- and 23-kD forms of TCR zeta are generated by specific ITAM phosphorylations. *Nature Immunol.* **1**, 322–328 (2000).
11. Iwashima, M. *et al.* Sequential interactions of the TCR with two distinct cytoplasmic tyrosine kinases. *Science* **263**, 1136–1139 (1994).
12. Zhang, W., Sloan-Lancaster, J., Kitchen, J., Trible, R. P. & Samelson, L. E. LAT: the ZAP-70 tyrosine kinase substrate that links T cell receptor to cellular activation. *Cell* **92**, 83–92 (1998).
13. Rincon, M. MAP-kinase signaling pathway in T cells. *Curr. Opin. Immunol.* **13**, 339–345 (2001).
14. Noraz, N. *et al.* Alternative antigen receptor (TCR) signaling in T cells derived from ZAP-70-deficient patients expressing high levels of Syk. *J. Biol. Chem.* **275**, 15832–15838 (2000).
15. Murphy, K. M., Heimberger, A. B. & Loh, D. Y. Induction by antigen of intrathymic apoptosis of CD4$^+$CD8$^+$TCR^{lo} thymocytes *in vivo*. *Science* **250**, 1720–1723 (1990).
16. Kisielow, P., Bluthmann, H., Staerz, U. D., Steinmetz, M. & von Boehmer, H. Tolerance in T-cell-receptor transgenic mice involves deletion of nonmature CD4$^+$8$^+$ thymocytes. *Nature* **333**, 742–746 (1988).
17. Kisielow, P., Teh, H. S., Bluthmann, H. & von Boehmer, H. Positive selection of antigen-specific T cells in thymus by restricting MHC molecules. *Nature* **335**, 730–733 (1988).
18. Wiest, D. L. *et al.* A spontaneously arising mutation in the DLAARN motif of murine ZAP-70 abrogates kinase activity and arrests thymocyte development. *Immunity* **6**, 663–671 (1997).
19. Sakaguchi, S., Sakaguchi, N., Asano, M., Itoh, M. & Toda, M. Immunologic self-tolerance maintained by activated T cells expressing IL-2 receptor α-chains (CD25). Breakdown of a single mechanism of self-tolerance causes various autoimmune diseases. *J. Immunol.* **155**, 1151–1164 (1995).
20. Keffer, J. *et al.* Transgenic mice expressing human tumor necrosis factor: a predictive genetic model of arthritis. *EMBO J.* **10**, 4025–4031 (1991).
21. Kouskoff, V. *et al.* Organ-specific disease provoked by systemic autoimmunity. *Cell* **87**, 811–822 (1996).
22. Pals, S. T., Radaszkiewicz, T., Roozendaal, L. & Gleichman, E. Chronic progressive polyarthritis and other symptoms of collagen vascular disease induced by graft-versus-host reaction. *J. Immunol.* **134**, 1475–1482 (1985).
23. Nishimura, H., Nose, M., Hiai, H., Minato, N. & Honjo, T. Development of lupus-like autoimmune diseases by disruption of the PD-1 gene encoding an ITIM motif-carrying immunoreceptor. *Immunity* **11**, 141–151 (1999).
24. Horai, R. *et al.* Development of chronic inflammatory arthropathy resembling rheumatoid arthritis in interleukin 1 receptor antagonist-deficient mice. *J. Exp. Med.* **191**, 313–320 (2000).
25. Atsumi, T. *et al.* A point mutation of Tyr-759 in interleukin 6 family cytokine receptor subunit gp130 causes autoimmune arthritis. *J. Exp. Med.* **196**, 979–990 (2002).
26. Dayer, J. M. & Burger, D. Cytokines and direct cell contact in synovitis: relevance to therapeutic intervention. *Arthritis Res.* **1**, 17–20 (1999).
27. Naka, T., Nishimoto, N. & Kishimoto, T. The paradigm of IL-6: from basic science to medicine. *Arthritis Res.* **4** (Suppl. 3), S233–S242 (2002).
28. Werlen, G., Hausmann, B., Naeher, D. & Palmer, E. Signaling life and death in the thymus: timing is everything. *Science* **299**, 1859–1863 (2003).
29. Nambiar, M. P. *et al.* T cell signalling abnormalities in systemic lupus erythematosus are associated with increased mutations/polymorphisms and splice variants of T cell receptor zeta chain messenger RNA. *Arthritis Rheum.* **44**, 1336–1350 (2001).
30. Takeuchi, T. *et al.* TCR zeta chain lacking exon 7 in two patients with systemic lupus erythematosus. *Int. Immunol.* **10**, 911–921 (1998).

Supplementary Information accompanies the paper on **www.nature.com/nature**.

Acknowledgements We thank H. von Boemer for transgenic mice; M. Singh (GBF, Germany) for a gift of recombinant HSP-70 through the support of the UNDP/World Bank/WHO Special Program for Research and Training on Tropical Diseases; F. Melchers, R. Zinkernagel, K. Yamamoto, R. Suzuki and Z. Fehervari for discussion; A. Kosugi and T. Nakayama for reagents; and E. Moriizumi for immunohistochemistry and histology. This work was supported by grants-in-aid from the Ministry of Education, Science, Sports and Culture, the Ministry of Human Welfare, Japan Science and Technology Corporation, and the Organization for Pharmaceutical Safety and Research of Japan.

Authors' contributions The SKG strain was established by S.S. and N.S. The experiments in Figs 1, 2a–d, 3f–h, 4, Supplementary Figs 1, 4 and 6 were conducted by N.S. and S.S.; those in Fig. 2b–d by Ta.T., N.S., H.H., To.T., S.Y., T. S., S.N. and S.S.; those in Figs 2e, f, 3a–c, e and Supplementary Fig. 2 by Ta.T.; that in Fig. 3d by To.T.; that in Supplementary Fig. 3 by T.N., and that in Supplementary Fig. 5 by T.M. ZAP-70-deficient mice were provided by I.N.

Competing interests statement The authors declare that they have no competing financial interests.

Correspondence and requests for materials should be addressed to S.S. (shimon@frontier.kyoto-u.ac.jp).

A positive-feedback-based bistable 'memory module' that governs a cell fate decision

Wen Xiong & James E. Ferrell Jr

Department of Molecular Pharmacology, Stanford University School of Medicine, Stanford, California 94305-5174, USA

The maturation of *Xenopus* oocytes can be thought of as a process of cell fate induction, with the immature oocyte representing the default fate and the mature oocyte representing the induced fate[1,2]. Crucial mediators of *Xenopus* oocyte maturation, including the p42 mitogen-activated protein kinase (MAPK) and the cell-division cycle protein kinase Cdc2, are known to be organized into positive feedback loops[3]. In principle, such positive feedback loops could produce an actively maintained 'memory' of a transient inductive stimulus and could explain the irreversibility of maturation[3–6]. Here we show that the p42 MAPK and Cdc2 system normally generates an irreversible biochemical response from a transient stimulus, but the response becomes transient when positive feedback is blocked. Our results explain how a group of intrinsically reversible signal transducers can generate an irreversible response at a systems level, and show how a cell fate can be maintained by a self-sustaining pattern of protein kinase activation.

Immature *Xenopus* oocytes are arrested in a G2-like phase of the cell cycle. In response to steroid hormones, the oocyte is released

ARTHRITIS & RHEUMATISM
Vol. 50, No. 8, August 2004, pp 2450–2458
DOI 10.1002/art.20367

Induction of RANKL Expression and Osteoclast Maturation by the Binding of Fibroblast Growth Factor 2 to Heparan Sulfate Proteoglycan on Rheumatoid Synovial Fibroblasts

Kazuhisa Nakano, Yosuke Okada, Kazuyoshi Saito, and Yoshiya Tanaka

Objective. **Rheumatoid arthritis (RA) is characterized by progressive joint destruction. The aim of this study was to clarify the relevance of RA synovial fibroblasts (RASFs) and fibroblast growth factor 2 (FGF-2), which is produced abundantly by RASFs, to the osteoclastogenesis and bone resorption in RA.**

Methods. **Synovial fibroblasts were prepared from the synovial tissues of 10 patients with active RA and 7 patients with osteoarthritis (OA). The expression of RANKL, intercellular adhesion molecule 1 (ICAM-1), FGF receptor 1 (FGFR-1), and heparan sulfate proteoglycan (HSPG) on synovial fibroblasts was measured by FACScan. Osteoclast formation in cocultures of RASFs and peripheral blood mononuclear cells (PBMCs) was evaluated by tartrate-resistant acid phosphatase staining and a pit-formation assay using dentin slices.**

Results. **FGF-2 induced the expression of both RANKL and ICAM-1 on RASFs more so than on OA synovial fibroblasts (OASFs). FGF-2–induced up-regulation of RANKL and ICAM-1 was inhibited by anti–FGF-2 antibody. Although FGFR-1 was equally expressed on RASFs and OASFs, HSPG was highly expressed on RASFs. Up-regulation of RANKL by FGF-2 on RASFs was diminished by the removal of heparan sulfate with heparitinase. Osteoclast formation from PBMCs induced by RASFs was inhibited by the addition of either heparitinase, anti–ICAM-1 antibody, anti–FGF-2 antibody, or osteoprotegerin. FGF-2–induced RANKL on RASFs and osteoclast formation were suppressed by an inhibitor of ERK.**

Conclusion. **FGF-2 was transferred to FGFR-1 through binding to HSPG, which is characteristically expressed on RASFs, resulting in RANKL- and ICAM-1–mediated maturation of osteoclasts via ERK activation. Thus, we propose that FGF-2 not only augments the proliferation of RASFs, but also is involved in osteoclast maturation, which leads to bone destruction in RA.**

Rheumatoid arthritis (RA) is an autoimmune disease characterized by progressive joint destruction that results from inflammation of multiple synovial joints. Destruction of bone and cartilage is one of the most serious problems in RA patients. Although histologic analyses have demonstrated that osteoclastic bone resorption at the bone–pannus interface is increased in RA joints (1), the mechanism has not yet been clarified. Since it has been reported that synovial cells from RA patients are capable of developing into osteoclasts (2), it is possible that the synovial tissue environment regulates osteoclastogenesis and results in joint destruction.

Fibroblast growth factor 2 (FGF-2) is a member of the family of heparin-binding cytokines with potent mitogenic effects on a variety of cells of mesodermal and ectodermal origin (3). FGF-2 has been reported to stimulate bone resorption in bone organ cultures (4), as well as osteoclastogenesis in a mouse bone marrow culture (5). Furthermore, it has been reported that among several bone-resorptive cytokines, only the FGF-2 concentration in the synovial fluid of RA patients was positively correlated with the severity of joint destruction (6). Recently, Yamashita et al (7) showed that

Kazuhisa Nakano, MD, Yosuke Okada, MD, Kazuyoshi Saito, MD, Yoshiya Tanaka, MD: University of Occupational and Environmental Health, Kitakyushu, Japan.

Address correspondence and reprint requests to Yoshiya Tanaka, MD, First Department of Internal Medicine, School of Medicine, University of Occupational and Environmental Health, 1-1 Iseigaoka Yahatanishi-ku, Kitakyushu, 807-8555 Japan. E-mail: tanaka@med.uoeh-u.ac.jp.

Submitted for publication June 18, 2003; accepted in revised form March 29, 2004.

anti–FGF-2–neutralizing antibody inhibited bone destruction in the joints of rats with adjuvant-induced arthritis, suggesting that the control of FGF-2 may prove to be therapeutically useful for RA. However, FGF-2 requires the presence of heparan sulfate proteoglycans (HSPGs) to bind FGF receptor (FGFR). HSPGs are coreceptors for FGF-2 and strongly promote the binding of FGF to FGFR and the subsequent activation of the receptor (8–10). Recent genetic studies in *Drosophila* provided compelling evidence that HSPGs are essential for FGF signaling in vivo (11).

The present study was designed to determine the role of FGF-2 and HSPG in the osteoclastogenesis that occurs in patients with RA. Our results showed that FGF-2/HSPG binding may provide powerful tools for inhibiting bone destruction in RA.

MATERIALS AND METHODS

Cell cultures. Synovial tissues were obtained from patients with active rheumatoid arthritis (12) and osteoarthritis (OA) (13), diagnosed according to the criteria of the American College of Rheumatology (formerly, the American Rheumatism Association), who were undergoing joint replacement surgery or synovectomy. Synovial tissues samples were dissected under sterile conditions in phosphate buffered saline (PBS), and immediately prepared for culture of fibroblast-like synovial cells.

Briefly, the tissue sample was minced into small pieces and digested with collagenase (Sigma-Aldrich Japan, Tokyo, Japan) in serum-free Dulbecco's modified Eagle's medium (DMEM; Gibco BRL, Grand Island, NY). After filtering through a nylon mesh, the cells were extensively washed, and suspended in DMEM, supplemented with 10% fetal calf serum (FCS; Bio-Pro, Karlsruhe, Germany). Finally, isolated cells were seeded in 25-cm^2 culture flasks (Falcon, Lincoln Park, NJ) and cultured in a humidified chamber with an atmosphere of 5% carbon dioxide. After overnight culture, nonadherent cells were removed, and incubation of adherent cells was continued in fresh medium. At confluence, the cells were trypsinized, passaged at a 1:3 split ratio, and recultured. The medium was changed twice each week, and the cells were used after 3–5 passages.

The study protocol was approved by the Ethics Review Committee of the University of Occupational and Environmental Health, School of Medicine. A signed consent form was obtained from each subject before tissue collection.

Reagents and monoclonal antibodies. FGF-2, osteoprotegerin (OPG) (PeproTech, London, UK), PD 98059, SB 202190 (both from Funakoshi, Tokyo, Japan), and chondroitinase ABC (Seikagaku, Tokyo, Japan) were purchased. Heparinase and heparitinase I and II were kindly donated by the Tokyo Research Institute of Seikagaku. Neutralizing antibodies against human FGF-2 produced in goats and nonimmune goat IgG were purchased from R&D Systems (Minneapolis, MN). The following monoclonal antibodies (mAb) were used as purified immunoglobulins in the preparation of synovial fibroblasts, staining, and analysis of cell surface molecules: anti–heparan sulfate mAb 10E4 (Seikagaku), anti-RANKL polyclonal antibody (C-20; Santa Cruz Biotechnology, Santa Cruz, CA), CD54 (ICAM-1) mAb 84H10 (kindly provided by S. Shaw, NIH, Bethesda, MD), anti-FGFR-1 antibody (Sigma-Aldrich Japan), fluorescein isothiocyanate (FITC)–conjugated donkey anti-goat IgG (Santa Cruz Biotechnology), and control mouse IgG1 (Becton Dickinson, San Jose, CA).

Fluorescence-activated cell sorting (FACS) analysis. Staining and flow cytometric analysis of osteoblasts and synovial cells were performed by standard procedures as described previously (14), using a FACScan (Becton Dickinson, Mountain View, CA). Briefly, cells (1×10^5) were incubated with specific mAb and subsequently with FITC-conjugated goat anti-mouse IgG antibody or rabbit anti-goat IgG antibody at saturating concentrations in FACS medium consisting of Hanks' balanced salt solution (Nissui, Tokyo, Japan), 0.5% human serum albumin (Green Cross, Osaka, Japan), and 0.2% NaN_3 (Sigma-Aldrich) for 30 minutes at 4°C. After 3 washes in FACS medium, the cells were analyzed with a FACScan. Amplification of the mAb binding was provided by a 3-decade logarithmic amplifier. Quantification of the cell surface antigens on one cell was performed using beads, QIFIKIT (Dako Japan, Kyoto, Japan).

Osteoclast formation in a coculture system of synovial fibroblasts and peripheral blood mononuclear cells (PBMCs). Subcultured synovial cells (3–5 passages) were composed of synovial fibroblasts, since all of the cells showed fibroblastoid morphology and were completely free of CD3-positive T cells and macrophages, as demonstrated by staining with CD11b or nonspecific esterase according to the method of Fujii et al (15).

PBMCs were derived from samples of peripheral blood using Ficoll-Paque. Briefly, peripheral blood was obtained from healthy donors, diluted 1:1 in PBS, layered onto Ficoll-Paque, and centrifuged at 400*g* for 20 minutes. The interface layer was washed 3 times in PBS and was used as PBMCs. Isolated PBMCs (4×10^5 cells/well) were resuspended in α-minimum essential medium (α-MEM) containing 10% FCS and 50 ng/ml of macrophage colony-stimulating factor (M-CSF) and then seeded in 48-well tissue culture plates (Costar 3548; Corning, Corning, NY). Three days later, adherent cells were used for subsequent cocultures with fibroblasts.

Synovial fibroblasts were added to 48-well plates (1×10^4 cells/well) and cocultured for 9 days in α-MEM containing 10% FCS, 50 ng/ml of M-CSF, and $10^{-7}M$ 1,25-dihydroxyvitamin D_3 ($1,25[OH]_2D_3$). After 9 days of culture, some dishes were stained for tartrate-resistant acid phosphatase (TRAP) as described previously (16); the other dishes were trypsinized and seeded onto dentin slices (4 mm). TRAP-positive multinucleated cells that contained more than 3 nuclei were identified as osteoclasts, and these were counted by light microscopy. On day 11, the dentin slices were placed in NH_4OH (1*N*) for 30 minutes and then cleaned by ultrasonication to remove adherent cells. The dentin slices were then washed with distilled water and stained with hematoxylin and eosin. Bone resorption was evaluated by scanning the area of resorption pits by light microscopy.

Statistical analysis. All data were expressed as the mean ± SD. Differences between groups were examined for statistical significance using the unpaired *t*-test. A *P* value less than 0.05 was considered statistically significant.